Journal of Applied Sciences

ISSN 1812-5654

science alert

ANSInet
an open access publisher
http://ansinet.com

Journal of Applied Sciences 6 (11): 2334-2357, 2006
ISSN 1812-5654

The P-version Finite Element Method Usimg Bezier-Bernstein Functions for Frames, Shells and Solids

[1]Nadir Boumechra and [2]Djamel Eddine Kerdal
[1]Département de Génie civil, Faculté des Sciences de l'Ingénieur,
Université Abou-Bekr Belkaïd, Tlemcen, Algérie
[2]Département de Génie civil, Faculté de Génie civil et de l'architecture,
Université des Sciences et de la Technologie d'Oran, Oran, Algérie

Abstract: In this study Bézier functions have used as displacement functions for frames, shells and solids. These polynomial shape functions have many mathematic and numerical advantages. The frame, shell and solid finite elements formed by Bézier functions are developed in p-version finite element method as non-discrete field. The Bézier parameterization properties treat more easily the geometrical boundary conditions or elements connection. The stiffness matrix, mass matrix, stability matrix and load vector of an isoparametric element can be related to the physical coordinates. The conditioning of the stiffness matrix for a frame element and the stiffness matrix forms of connected elements are presented. The numerical results converge to the exact solutions in a faster rate than the usual finite elements using the same number of degrees of liberty. A number of examples are given for demonstration.

Key words: Bézier functions, finite element method, p-version, frame, shell, solid, static, vibration, buckling

INTRODUCTION

A great variety of approximation functions have been used in the last decades for performing geometrical design and mechanical analysis. Trigonometric and polynomial functions are the most used ones. Polynomials are a useful mathematical tools as they are simply defined, can be calculated quickly on computer and represent an extraordinary variety of functions. The first approximation polynomials are been based on Hermite or Lagrange functions family, used in the simple or higher order finite elements.

A new concept of a hierarchical shape functions has been proposed by Peano (1975) using the Legendre polynomials. These have the hierarchical and orthogonal properties of p-order polynomials. Consequently, it is easy to construct adaptive computations in any finite element analysis.

The B-Spline functions are used in the analyses of beam, plate and shell problems. The majority of these works use a cubic spline functions so called B3-spline functions (Antes, 1974). It is also possible to expand the shape function into p-degree B-Spline series (Kagan *et al.*, 1998). A new approach using high – order of splines with duplication of some knots and called a non – discrete approach of spline finite element method is suggested (Fujiu, 1981). This method accelerates the convergence of numerical results and treats easily different geometrical boundary conditions. It has been employed to analyze many static, vibration and buckling problems of frames, plates and shells successfully.

P. Bézier in 1982 proposed a specific polynomial curves in computer aided geometric design (CAGD) for the car industry (Demengel and Pouget, 1998). The definition of Bézier curves or Bézier functions is based on Bernstein polynomials family. A Bézier function of degree n is defined by a sequence of n+1 control points blending with Bernstein polynomials. It takes full advantage of its stability when several other polynomials interpolation becomes increasingly ill-conditioned as the polynomial degree n increases (Farouki, 1981 and Hermann, 1996). The Bézier function is used most frequently in computer graphics and geometric modelling; often using the triangular Bézier patches (Farin, 1997; Barth and Stuzlinger, 1993).

In this study we describe the mathematical properties of Bézier functions and their relations with B-Spline functions. We develop the Bézier functions as the displacement functions in frames, shells and solids isoparametric finite elements. The conditioning number of

Corresponding Author: Nadir Boumechra, Département de Génie civil, Faculté des Sciences de l'Ingénieur,
Université Abou-Bekr Belkaïd, Chetouane, Tlemcen, Algérie
Tel: 00-213- 43 28 65 93, 00-213- 71 72 51 17 Fax: 00-213- 43 20 37 19

the stiffness matrix is evaluated and compared to other polynomials approximation. In this study we shall consider only one-dimensional p-version functions. The stiffness, masses and stability matrix and force vector are developed. The global matrices and vectors are constructed by a matrix transformation procedure to satisfy displacements compatibility along the interfaces of elements. Then the Bézier finite element approach is used to solve static, dynamic and stability problems of frames, shells and solides structures. Several numerical examples prove that a good convergence of the results is obtained by increasing the Bézier finite element orders.

BEZIER FUNCTIONS

The Bézier functions represent a parametric function. It is written as:

$$f(x) = \sum_{i=1}^{m} p_i . B_{m,i}(x) \text{ with } x \in [0,1] \tag{1}$$

where p_i are the control points and $B_{m,i}(x)$ are the blending functions called the Bernstein polynomials of degree (m-1) with the following forms (Fig. 1):

$$B_{m,i}(x) = C_{i-1}^{m-1} . (1-x)^{m-i} . (x)^{i-1} \qquad i = 1,m \tag{2}$$

where C_{i-1}^{m-1} are the binomial coefficients, i.e.,

$$C_{i-1}^{m-1} = \binom{m-1}{i-1} = \frac{(m-1)!}{(m-i)!.(i-1)!} \tag{3}$$

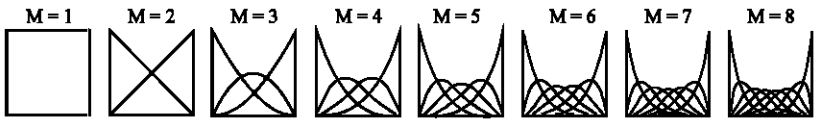

Fig. 1: Typical Bernstein polynomials for m = 1,8

The geometrical representation of the first eight derivatives of $B_{m,i}(X)$ is shown in Fig. 2.

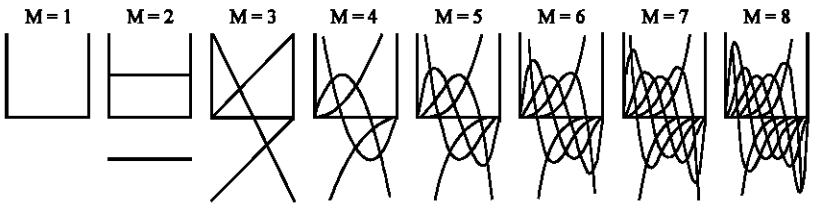

Fig. 2: The first derivative of Bernstein polynomials for m = 1,8

The Bernstein functions have the following properties:

- Non-negativity: $B_{m,i}(x) \geq 0 \qquad \forall x \in [0,1]$ (4a)
- Partition of unity: $\sum_{i=1}^{m} B_{m,i}(x) = 1 \quad \forall x \in [0,1]$ (4b)
- Symmetry: $B_{m,i}(x) = B_{m,m-i+1}(1-x) \qquad \forall x \in [0,1]$ for all i = 1,m (4c)
- Interpolation: $B_{m,i}(0) = \delta_{1,i}$ and $B_{m,i}(1) = \delta_{i,m}$ (4d)

- Recursive relation: $B_{m+1,i}(x) = (1-x).B_{m,i}(x) + (x).B_{m,i-1}(x)$ (4e)
- Uni-modality: $Max_{0\le x\le 1}(B_{m,i}(x))$ occurs at $x = (i-1)/(m-1)$ (4f)
- Linear independence: $\sum_{i=1}^{m} p_i.B_{m,i}(x) = 0 \Leftrightarrow c_i = 0$ for all i = 1,m (4g)
- Converting from power basis to Bernstein basis gives $x^k = \sum_{i=k+1}^{m} \frac{\binom{i-1}{k}}{\binom{m-1}{k}}.B_{m,i}(x)$ (4h)
- Derivatives: $\frac{\partial}{\partial x}\left(B_{m,i}(x)\right) = m.\left(B_{m-1,i-1}(x) - B_{m-1,i}(x)\right)$ (4i)
- Integration: $\int_0^1 B_{m,i}(x) = \frac{1}{m}$ for all i = 1,m (4j)

Another advantage of the Bernstein form, of much broader significance, is its numerical stability as a representation for polynomials over finite intervals.

We note that the Bézier-Bernstein function are also called B-Spline function of Bézier with multiple knots which are generated by superposing m adjoining knots of B-Splines of order m at the ends (Demengel and Pouget, 1998). We recall the recurrence formulae proposed by Cox and De Boor for B-Splines practical evaluation (Fujii, 1982):

$$N_{m,i}(x) = \frac{(x - x_i)}{(x_{m+i-1} - x_i)}.N_{m-1,i}(x) + \frac{(x_{m+i} - x)}{(x_{m+i} - x_{i+1})}.N_{m-1,i+1}(x) \quad (5)$$

starting from the initial value: $N_{1,i}(x) = 1$ for $x_i \le x \le x_{i+1}$ (6)

THE P-VERSION BEZIER FINITE ELEMENT METHOD

In the coordinate relationships, the shape function can be specified in local coordinates (ξ, η, ζ) and by suitable transformations the element properties established in global system (x,y,z). All deformation-displacement, stress-deformation relations, energy, Jacobian matrix and all representative matrices of an isoparametric finite element are expressed in the local coordinates corresponding of global coordinates.

Corresponding to a new local interval [-1, +1], then a simple transformation of the Bernstein polynomials is made as:

$$B_{m,i}(\xi) = \binom{m-1}{i-1}.\left(\frac{1}{2} - \frac{\xi}{2}\right)^{m-i}.\left(\frac{1}{2} + \frac{\xi}{2}\right)^{i-1} \quad (7)$$

Thus isoparametric finite elements of the basic one-, two-or three-dimensional types are presented into irregular forms as shown in Fig. 3.

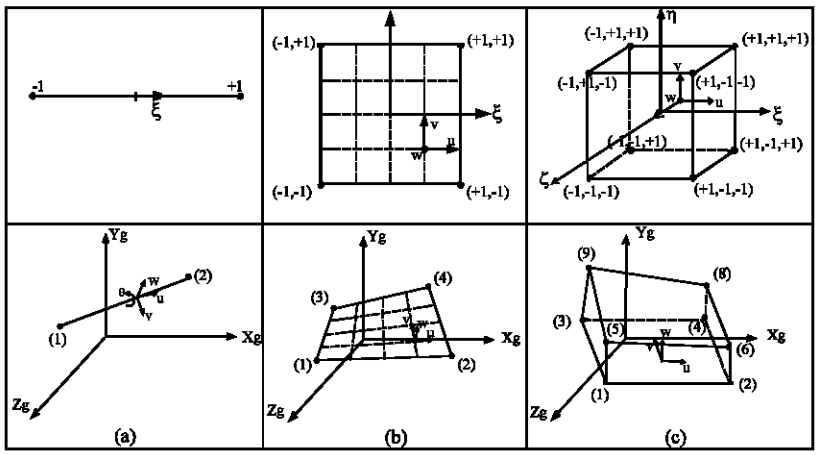

Fig. 3: Representation of the isoparametric finite elements in local and global coordinates.
a- One-dimensional element, b- Two-dimensional element, c- Three-dimensional element

The isoparametric frame finite element: In the frame finite element, the axial displacement u, the transverse displacements v and w and the normal rotation can be expressed at position ξ (Fig. 3a). The displacement function {f} is taken as summation of 'm' Bernstein polynomials as follows:

$$\{f\}=\begin{Bmatrix}u\\v\\w\\\theta\end{Bmatrix}=\begin{Bmatrix}\sum_{i=1}^{mu}u_i.B_{mu,i}(\xi)\\\sum_{i=1}^{mv}v_i.B_{mv,i}(\xi)\\\sum_{i=1}^{mw}w_i.B_{mw,i}(\xi)\\\sum_{i=1}^{m\theta}\theta_i.B_{m\theta,i}(\xi)\end{Bmatrix}=\begin{bmatrix}B_{mu,i}(\xi) & B_{mv,i}(\xi) & B_{mw,i}(\xi) & B_{m\theta,i}(\xi)\end{bmatrix}.\begin{Bmatrix}u_i\\v_i\\w_i\\\theta_i\end{Bmatrix}=[N].\{\delta\} \tag{8}$$

where (u_i,v_i,w_i,θ_i) are the displacement-control points to be determined and $B_{mu,i}(\xi)$, $B_{mv,i}(\xi)$, $B_{mw,i}(\xi)$ and $B_{m\theta,i}(\xi)$ are the Bernstein polynomials corresponding to the frame displacements.

The Isoparametric shell finite element: In the shell finite element, the displacement is defined in local coordinates ξ and η by membrane displacements u, v and the flexural displacement w (Fig. 3b). The displacement function is taken as summation of "m" Bernstein polynomials by:

$$\{f\}=\begin{Bmatrix}u\\v\\w\end{Bmatrix}=\begin{Bmatrix}\sum_{i=1}^{mu}\sum_{j=1}^{nu}u_{ij}.B_{mu,i}(\xi).B_{nu,j}(\eta)\\\sum_{i=1}^{mv}\sum_{j=1}^{nv}vij.B_{mv,i}(\xi).B_{nv,j}(\eta)\\\sum_{i=1}^{mw}\sum_{j=1}^{nw}w_{ij}.B_{mw,i}(\xi).B_{nw,j}(\eta)\end{Bmatrix}=\begin{bmatrix}\left[B_{mu,i}(\xi).B_{nu,j}(\eta)\right] & [0] & [0]\\[0] & \left[B_{mv,i}(\xi).B_{nv,j}(\eta)\right] & [0]\\[0] & [0] & \left[B_{mw,i}(\xi).B_{nw,j}(\eta)\right]\end{bmatrix}\begin{Bmatrix}u_{ij}\\v_{ij}\\w_{ij}\end{Bmatrix}=[N].\{\delta\} \tag{9}$$

where (u_{ij}, v_{ij}, w_{ij}) are the bi-dimensional displacement – control points to be determined and $B_{mu,i}(\xi)$, $B_{nu,j}(\eta)$, $B_{mv,i}(\xi)$, $B_{nv,j}(\eta)$, $B_{mw,i}(\xi)$ and $B_{nw,j}(\eta)$ are the Bernstein polynomials corresponding to the shell's displacements.

The Isoparametric solid finite element: The u, v and w displacements in the solid finite element are defined in local coordinates ξ, η and ζ (Fig. 3c). The displacement functions are taken as the summation of "m" Bernstein polynomials by:

$$\{f\}=\begin{Bmatrix}u\\v\\w\end{Bmatrix}=\begin{Bmatrix}\sum_{i=1}^{mu}\sum_{j=1}^{nu}\sum_{k=1}^{lu}u_{ijk}.B_{mu,i}(\xi).B_{nu,j}(\eta).B_{lu,k}(\zeta)\\\sum_{i=1}^{mv}\sum_{j=1}^{nv}\sum_{k=1}^{lv}v_{ijk}.B_{mv,i}(\xi).B_{nv,j}(\eta).B_{lv,k}(\zeta)\\\sum_{i=1}^{mw}\sum_{j=1}^{nw}\sum_{k=1}^{lw}w_{ijk}.B_{mw,i}(\xi).B_{nw,j}(\eta).B_{lw,k}(\zeta)\end{Bmatrix}=$$

$$=\begin{bmatrix}\left[B_{mu,i}(\xi).B_{nu,j}(\eta).B_{lu,k}(\zeta)\right] & [0] & [0]\\[0] & \left[B_{mv,i}(\xi).B_{nv,j}(\eta).B_{lv,k}(\zeta)\right] & [0]\\[0] & [0] & \left[B_{mw,i}(\xi).B_{nw,j}(\eta).B_{lw,k}(\zeta)\right]\end{bmatrix}\begin{Bmatrix}u_{ijk}\\v_{ijk}\\w_{ijk}\end{Bmatrix}=[N].\{\delta\} \tag{10}$$

where $(u_{ijk}, v_{ijk}, w_{ijk})$ are the tri-dimensional displacement-control points to be determined and $B_{mu,i}(\xi)$, $B_{nu,j}(\eta)$, $B_{lu,k}(\zeta)$, $B_{mv,i}(\xi)$, $B_{nv,j}(\eta)$, $B_{lv,k}(\zeta)$, $B_{mw,i}(\xi)$, $B_{nw,j}(\eta)$ and $B_{lw,k}(\zeta)$ are the Bernstein polynomials corresponding to the solid's displacements u, v and w.

Analysis of structures: In the linear analysis of structures, the static, modal and buckling problems are studied. For frame, shell or solid isoparametric finite elements, the stiffness, mass, stability matrices and load vectors can be obtained by finite element method using energy principles. Then the typical matrix equations of each analysis are shown as follows:

$$\text{Static analysis: } [K]\cdot\{\delta\} = \{F\} \tag{11}$$

$$\text{Modal analysis: } ([K]-\omega^2\cdot[M])\cdot\{\delta\} = \{0\} \tag{12}$$

$$\text{Buckling analysis: } ([K]-\lambda\cdot\{\delta\} = \{0\}) \tag{13}$$

where [K], [M] and [G] are the stiffness, mass and stability matrix respectively. {F} and {δ} are the load vector and the displacement – control points vector. The constant ω is the natural circular and λ is the buckling load vector.

Therefore it is possible to choose any different polynomial degrees for the Bezier-Bernstein displacement functions in each local direction separately.

The details of finite element matrices are given in Appendix.

For the static analysis, the system of equations is solved by using banded Gaussian elimination, without pivoting. For the modal and buckling analysis, the eigen-value problem is solved using Householder – Sturm sequence and Inverse iteration method.

APPENDIX

Technical details of Bézier F.E.M.

The Isoparametric frame finite element: The strain-displacement relationship will be:

$$\{\varepsilon\} = \begin{Bmatrix}\varepsilon_u\\ \varepsilon_\theta\end{Bmatrix} = \begin{bmatrix} \dfrac{\partial B_{mu,1}(\xi)}{\partial\xi} & -y_1.\dfrac{\partial^2 B_{mv,1}(\xi)}{\partial\xi} & -z_1.\dfrac{\partial^2 B_{mw,1}(\xi)}{\partial\xi} & 0 \\ 0 & 0 & 0 & \dfrac{\partial B_{m\theta,1}(\xi)}{\partial\xi} \end{bmatrix}.\begin{Bmatrix}u_1\\ v_1\\ w_1\\ \theta_1\end{Bmatrix} = [B].\{\delta\} \tag{A1}$$

where y_1 and z_1 are the locale coordinates of the frame's cross-section.

The linear stress-strain relationship is: $\{\sigma\} = \begin{Bmatrix}\sigma_u\\ \sigma_\theta\end{Bmatrix} = \begin{bmatrix}E & 0\\ 0 & G\end{bmatrix}.\begin{Bmatrix}\varepsilon_u\\ \varepsilon_\theta\end{Bmatrix} = [C].\{\varepsilon\}$ (A2)

where E and G are the Young's modulus and shear modulus respectively.

Consequently of developing the total energy, the stiffness matrix [K] can be evaluated from:

$$[K] = \begin{bmatrix} E.\begin{bmatrix} A.\left[\int_{-1}^{+1}\dfrac{\partial B_{mu,1}(\xi)}{\partial\xi}.\dfrac{\partial B_{mu,J}(\xi)}{\partial\xi}.d\xi\right] & [0] & [0] \\ [0] & I_{Y'}.\left[\int_{-1}^{+1}\dfrac{\partial^2 B_{mv,1}(\xi)}{\partial\xi}.\dfrac{\partial^2 B_{mv,J}(\xi)}{\partial\xi}.d\xi\right] & [0] \\ [0] & [0] & I_Z.\left[\int_{-1}^{+1}\dfrac{\partial^2 B_{mw,1}(\xi)}{\partial\xi}.\dfrac{\partial^2 B_{mw,J}(\xi)}{\partial\xi}.d\xi\right] \end{bmatrix} & \begin{bmatrix}[0]\\ [0]\\ [0]\end{bmatrix} \\ [[0]\ \ [0]\ \ [0]] & G.J.\left[\int_{-1}^{+1}\dfrac{\partial B_{m\theta,1}(\xi)}{\partial\xi}.\dfrac{\partial B_{m\theta,J}(\xi)}{\partial\xi}.d\xi\right] \end{bmatrix}.\det J \tag{A3}$$

where A, I_x, I_y and J are the cross-sectional area, flexural inertias and tortional inertia respectively. The Jacobian determinant detJ of frame element is equal to half of its length.

The load vector for uniform loading in a Bézier-Bernstein construction is:

$$\{F\} = \det J.\left[\int q_u(\xi).B_{mu,1}(\xi).d\xi \quad \int q_v(\xi).B_{mv,1}(\xi).d\xi \quad \int q_w(\xi).B_{mw,1}(\xi).d\xi \quad [0]\right]^T \tag{A4}$$

The load vector for punctual loading is:

$$\{F\} = \left[Q_u B_{mu,1}(\xi_0) \quad Q_v B_{mv,1}(\xi_0) \quad Q_w B_{mw,1}(\xi_0) \quad [0]\right]^T \tag{A5}$$

Similarly the mass matrix for a frame finite element with mass per unit volume ρ is given by:

$$[M] = \rho.A.\begin{bmatrix} \left[\int B_{mu,1}(\xi).B_{mu,j}(\xi).d\xi\right] & [0] & [0] & [0] \\ [0] & \left[\int B_{mv,1}(\xi).B_{mv,j}(\xi).d\xi\right] & [0] & [0] \\ [0] & [0] & \left[\int B_{mw,1}(\xi).B_{mw,j}(\xi).d\xi\right] & [0] \\ [0] & [0] & [0] & [0] \end{bmatrix}.\det J \tag{A6}$$

The stability matrix corresponding to a longitudinal compressive force N_0 is:

$$[G] = N_0.\begin{bmatrix} \left[\int \frac{\partial B_{mu,1}(\xi)}{\partial \xi}.\frac{\partial B_{mu,j}(\xi)}{\partial \xi}.d\xi\right] & [0] & [0] & [0] \\ [0] & \left[\int \frac{\partial B_{mv,1}(\xi)}{\partial \xi}.\frac{\partial B_{mv,j}(\xi)}{\partial \xi}.d\xi\right] & [0] & [0] \\ [0] & [0] & \left[\int \frac{\partial B_{mw,1}(\xi)}{\partial \xi}.\frac{\partial B_{mw,j}(\xi)}{\partial \xi}.d\xi\right] & [0] \\ [0] & [0] & [0] & [0] \end{bmatrix}.\det J \tag{A7}$$

The Isoparametric shell finite element: In the membrane-flexural states of shell behaviour, the strain-displacement equation will be:

$$\{\varepsilon\} = \left\{[\varepsilon_M]^T [\varepsilon_F]^T\right\} = \left\{\left[\left(\frac{\partial u}{\partial x_L}\right) \left(\frac{\partial v}{\partial y_L}\right) \left(\frac{\partial u}{\partial y_L} + \frac{\partial v}{\partial x_L}\right)\right]^T \left[\left(-\frac{\partial^2 w}{\partial x_L^2}\right) \left(-\frac{\partial^2 w}{\partial y_L^2}\right) \left(2.\frac{\partial^2 w}{\partial x_L \partial y_L}\right)\right]^T\right\} \tag{A8}$$

where x_L, y_L are the local orthogonal coordinates of the finite element to be defined at an appropriate direction.

It is necessary to develop the chain rule using a corresponding Jacobian matrix, which can write the relations between the isoparametric reference system (ξ,η) and local orthogonal coordinates (x_L, y_L). We must also establish a relation between local orthogonal coordinates (x_L, y_L) and global coordinates (x,y,z).

The linear stress-strain relationships for the membrane and flexural finite element are:

$$\{\sigma_M\} = [\sigma_{XX} \quad \sigma_{YY} \quad \tau_{XY}]^T = [D_M].\{\varepsilon_M\} = [D_M].[B_M].\{\delta_M\} \tag{A9}$$

$$\{\sigma_F\} = [M_{XX} \quad M_{YY} \quad M_{XY}]^T = [D_F].\{\varepsilon_F\} = [D_F].[B_F].\{\delta_F\} \tag{A10}$$

The strain matrices $[B_M]$ and $[B_F]$ are derived by appropriate differentiation of equation (A9) and equation (A10) using equation (A8) respectively. The matrices $[D_M]$ and $[D_F]$ are the elasticity matrices defined for membrane and flexural behaviours respectively.

Consequently of developing the total energy of membrane and Kirchhoff's plate bending, the stiffness matrix [K] can be evaluated from:

$$[K]=\begin{bmatrix}[K_M] & [0]\\ [0] & [K_F]\end{bmatrix} \tag{A11}$$

The membrane and bending stiffness matrices $[K_M]$ and $[K_F]$ are defined as:

$$[K_M]=t.\int_{-1}^{+1}\int_{-1}^{+1}[B_M]^T.[D_M].[B_M].\det J(\xi,\eta).d\xi.d\eta$$

$$=t.\int_{-1}^{+1}\int_{-1}^{+1}\begin{bmatrix}\left[\frac{\partial B_{mu,i}(\xi)}{\partial\xi}.B_{nu,j}(\eta)\right]^T & \left[B_{mu,i}(\xi).\frac{\partial B_{nu,j}(\eta)}{\partial\eta}\right]^T & [0] & [0]\\ [0] & [0] & \left[\frac{\partial B_{mv,i}(\xi)}{\partial\xi}.B_{nv,j}(\eta)\right]^T & \left[B_{mv,i}(\xi).\frac{\partial B_{nv,j}(\eta)}{\partial\eta}\right]^T\end{bmatrix}.$$

$$\begin{bmatrix}\alpha_1 & 0 & \alpha_3\\ \alpha_2 & 0 & \alpha_4\\ 0 & \alpha_3 & \alpha_1\\ 0 & \alpha_4 & \alpha_2\end{bmatrix}.\begin{bmatrix}D_1 & D_2 & 0\\ D_2 & D_1 & 0\\ 0 & 0 & D_3\end{bmatrix}.\begin{bmatrix}\alpha_1 & \alpha_2 & 0 & 0\\ 0 & 0 & \alpha_3 & \alpha_4\\ \alpha_3 & \alpha_4 & \alpha_1 & \alpha_2\end{bmatrix}.$$

$$\begin{bmatrix}\left[\frac{\partial B_{mu,i}(\xi)}{\partial\xi}.B_{nu,j}(\eta)\right] & [0]\\ \left[B_{mu,i}(\xi).\frac{\partial B_{nu,j}(\eta)}{\partial\eta}\right] & [0]\\ [0] & \left[\frac{\partial B_{mv,i}(\xi)}{\partial\xi}.B_{nv,j}(\eta)\right]\\ [0] & \left[B_{mv,i}(\xi).\frac{\partial B_{nv,j}(\eta)}{\partial\eta}\right]\end{bmatrix}.\det J(\xi,\eta).d\xi.d\eta \tag{A12}$$

$$[K_F]=\frac{t^3}{12}.\int_{-1}^{+1}\int_{-1}^{+1}[B_F]^T.[D_F].[B_F].\det J(\xi,\eta).d\xi.d\eta$$

$$=\frac{t^3}{12}.\int_{-1}^{+1}\int_{-1}^{+1}\left[\left[\frac{\partial^2 B_{mw,i}(\xi)}{\partial\xi^2}.B_{nw,j}(\eta)\right]^T \left[\frac{\partial B_{mw,i}(\xi)}{\partial\xi}.B_{nw,j}(\eta)\right]^T \left[B_{mw,i}(\xi).\frac{\partial^2 B_{nw,j}(\eta)}{\partial\eta^2}\right]^T \left[B_{mw,i}(\xi).\frac{\partial B_{nw,j}(\eta)}{\partial\eta}\right]^T \left[\frac{\partial B_{mw,i}(\xi)}{\partial\xi}.\frac{\partial B_{nw,j}(\eta)}{\partial\eta}\right]^T\right]$$

$$\begin{bmatrix}-\alpha_1^2 & -\alpha_3^2 & 2.\alpha_1.\alpha_3\\ -\left(\alpha_1.\frac{\partial\alpha_1}{\partial\xi}+\alpha_2.\frac{\partial\alpha_1}{\partial\eta}\right) & -\left(\alpha_3.\frac{\partial\alpha_3}{\partial\xi}+\alpha_4.\frac{\partial\alpha_3}{\partial\eta}\right) & 2.\left(\alpha_1.\frac{\partial\alpha_3}{\partial\xi}+\alpha_2.\frac{\partial\alpha_3}{\partial\eta}\right)\\ -\alpha_2^2 & -\alpha_4^2 & 2.\alpha_2.\alpha_4\\ -\left(\alpha_1.\frac{\partial\alpha_2}{\partial\xi}+\alpha_2.\frac{\partial\alpha_2}{\partial\eta}\right) & -\left(\alpha_3.\frac{\partial\alpha_4}{\partial\xi}+\alpha_4.\frac{\partial\alpha_4}{\partial\eta}\right) & 2.\left(\alpha_1.\frac{\partial\alpha_4}{\partial\xi}+\alpha_2.\frac{\partial\alpha_4}{\partial\eta}\right)\\ -2.\alpha_1.\alpha_2 & -2.\alpha_3.\alpha_4 & 2.(\alpha_1.\alpha_4+\alpha_2.\alpha_3)\end{bmatrix}.\begin{bmatrix}D_1 & D_2 & 0\\ D_2 & D_1 & 0\\ 0 & 0 & D_3\end{bmatrix}.$$

$$\begin{bmatrix}-\alpha_1^2 & -\left(\alpha_1.\frac{\partial\alpha_1}{\partial\xi}+\alpha_2.\frac{\partial\alpha_1}{\partial\eta}\right) & -\alpha_2^2 & -\left(\alpha_1.\frac{\partial\alpha_2}{\partial\xi}+\alpha_2.\frac{\partial\alpha_2}{\partial\eta}\right) & -2.\alpha_1.\alpha_2\\ -\alpha_3^2 & -\left(\alpha_3.\frac{\partial\alpha_3}{\partial\xi}+\alpha_4.\frac{\partial\alpha_3}{\partial\eta}\right) & -\alpha_4^2 & -\left(\alpha_3.\frac{\partial\alpha_4}{\partial\xi}+\alpha_4.\frac{\partial\alpha_4}{\partial\eta}\right) & -2.\alpha_3.\alpha_4\\ 2.\alpha_1.\alpha_2 & 2.\left(\alpha_1.\frac{\partial\alpha_3}{\partial\xi}+\alpha_2.\frac{\partial\alpha_3}{\partial\eta}\right) & 2.\alpha_2.\alpha_4 & 2.\left(\alpha_1.\frac{\partial\alpha_4}{\partial\xi}+\alpha_2.\frac{\partial\alpha_4}{\partial\eta}\right) & 2.(\alpha_1.\alpha_4+\alpha_2.\alpha_3)\end{bmatrix}.\begin{bmatrix}\left[\frac{\partial^2 B_{mw,i}(\xi)}{\partial\xi^2}.B_{nw,j}(\eta)\right]\\ \left[\frac{\partial B_{mw,i}(\xi)}{\partial\xi}.B_{nw,j}(\eta)\right]\\ \left[B_{mw,i}(\xi).\frac{\partial^2 B_{nw,j}(\eta)}{\partial\eta^2}\right]\\ \left[B_{mw,i}(\xi).\frac{\partial B_{nw,j}(\eta)}{\partial\eta}\right]\\ \left[\frac{\partial B_{mw,i}(\xi)}{\partial\xi}.\frac{\partial B_{nw,j}(\eta)}{\partial\eta}\right]\end{bmatrix}.\det J(\xi,\eta).d\xi.d\eta \tag{A13}$$

$$\begin{bmatrix} \alpha_1 & \alpha_2 \\ \alpha_3 & \alpha_4 \end{bmatrix} = \begin{bmatrix} \left(\frac{\partial \xi}{\partial x_L}\right) & \left(\frac{\partial \eta}{\partial x_L}\right) \\ \left(\frac{\partial \xi}{\partial y_L}\right) & \left(\frac{\partial \eta}{\partial y_L}\right) \end{bmatrix} = J^{-1} \tag{A14}$$

where t is the thickness of a shell finite element, E is the Young's modulus and ν is the Poisson's ratio.

The equation (A14) defines the components of the inverse of Jacobian matrix J. For an isoparametric non-distorted shell finite element (α_1, α_2, α_3, α_4) are polynomials of second degree in (ξ,η) and the Jacobian determinant detJ is a polynomial of first degree.

The load vector for uniform or non-uniform surface loading is:

$$\begin{aligned} \{F\} = \Bigg[& \left[\iint_S q_\xi(\xi,\eta).B_{mu,i}(\xi).B_{nu,j}(\eta).\det J(\xi,\eta).d\xi.d\eta \right]^T \\ & \left[\iint_S q_\eta(\xi,\eta).B_{mv,i}(\xi).B_{nv,j}(\eta).\det J(\xi,\eta).d\xi.d\eta \right]^T \\ & \left[\iint_S q_\zeta(\xi,\eta).B_{mw,i}(\xi).B_{nw,j}(\eta).\det J(\xi,\eta).d\xi.d\eta \right]^T \Bigg]^T \end{aligned} \tag{A15}$$

We note that ζ is a local coordinate which is perpendicular to the coordinates of the shell element surface ξ and η. The load vector for punctual loading defined in a point with local coordinates (ξ_0, η_0) is:

$$\{F\} = \left[\left[P_\xi.B_{mu,i}(\xi_0).B_{nu,j}(\eta_0) \right]^T \quad \left[P_\eta.B_{mv,i}(\xi_0).B_{nv,j}(\eta_0) \right]^T \quad \left[P_\zeta.B_{mw,i}(\xi_0).B_{nw,j}(\eta_0) \right]^T \right]^T \tag{A16}$$

The mass matrix for a shell finite element with mass per unit volume ρ is given by:

$$[M] = \begin{bmatrix} [M_u] & [0] & [0] \\ [0] & [M_v] & [0] \\ [0] & [0] & [M_w] \end{bmatrix} \tag{A17}$$

The matrices $[M_u]$, $[M_u]$ and [Mw] are the mass matrices corresponding to the displacements u, v and w respectively.

$$[M_u] = \rho.t.\int_{-1}^{+1}\int_{-1}^{+1} \left[B_{mu,i}(\xi).B_{nu,j}(\eta) \right]^T . \left[B_{mu,i}(\xi).B_{nu,j}(\eta) \right].\det J(\xi,\eta).d\xi.d\eta \tag{A18a}$$

$$[M_v] = \rho.t.\int_{-1}^{+1}\int_{-1}^{+1} \left[B_{mv,i}(\xi).B_{nv,j}(\eta) \right]^T . \left[B_{mv,i}(\xi).B_{nv,j}(\eta) \right].\det J(\xi,\eta).d\xi.d\eta \tag{A18b}$$

$$[M_w] = \rho.t.\int_{-1}^{+1}\int_{-1}^{+1} \left[B_{mw,i}(\xi).B_{nw,j}(\eta) \right]^T . \left[B_{mw,i}(\xi).B_{nw,j}(\eta) \right].\det J(\xi,\eta).d\xi.d\eta \tag{A18c}$$

The stability matrix corresponding to a longitudinal compressive stress σ_{xl} is:

$$[G_{xl}] = t.\sigma_{xl}.\int_{-1}^{+1}\int_{-1}^{+1} \begin{bmatrix} (\alpha_1^2.G_{u,1} + \alpha_1.\alpha_2.(G_{u,2}+G_{u,3}) + \alpha_2^2.G_{u,4}) & [0] & [0] \\ [0] & (\alpha_1^2.G_{v,1} + \alpha_1.\alpha_2.(G_{v,2}+G_{v,3}) + \alpha_2^2.G_{v,4}) & [0] \\ [0] & [0] & (\alpha_1^2.G_{w,1} + \alpha_1.\alpha_2.(G_{w,2}+G_{w,3}) + \alpha_2^2.G_{w,4}) \end{bmatrix} .\det J(\xi,\eta).d\xi.d\eta \tag{A19}$$

The stability matrix corresponding to a transverse compressive stress σ_{yl} is:

$$\left[G_{yl}\right] = t.\sigma_{yl}.\int_{-1}^{+1}\int_{-1}^{+1}\begin{bmatrix} (\alpha_3^2.G_{u,1} + \alpha_3.\alpha_4.(G_{u,2}+G_{u,3}) + \alpha_4^2.G_{u,4}) & [0] & [0] \\ [0] & (\alpha_3^2.G_{v,1} + \alpha_3.\alpha_4.(G_{v,2}+G_{v,3}) + \alpha_4^2.G_{v,4}) & [0] \\ [0] & [0] & (\alpha_3^2.G_{w,1} + \alpha_3.\alpha_4.(G_{w,2}+G_{w,3}) + \alpha_4^2.G_{w,4}) \end{bmatrix}.\det J(\xi,\eta).d\xi.d\eta \quad \text{(A20)}$$

The stability matrix corresponding to a shear stress τ_{xyl} is:

$$\left[G_{xyl}\right] = 2.t.\tau_{xyl}.\int_{-1}^{+1}\int_{-1}^{+1}\begin{bmatrix} (\alpha_1.\alpha_3.G_{u,1} + (\alpha_1.\alpha_4+\alpha_2.\alpha_3).G_{u,2} + \alpha_2.\alpha_4.G_{u,4}) & [0] & [0] \\ [0] & (\alpha_1.\alpha_3.G_{v,1} + (\alpha_1.\alpha_4+\alpha_2.\alpha_3).G_{v,2} + \alpha_2.\alpha_4.G_{v,4}) & [0] \\ [0] & [0] & (\alpha_1.\alpha_3.G_{w,1} + (\alpha_1.\alpha_4+\alpha_2.\alpha_3).G_{w,2} + \alpha_2.\alpha_4.G_{w,4}) \end{bmatrix}.\det J(\xi,\eta).d\xi.d\eta \quad \text{(A21)}$$

where

$$\left[G_{u,1}\right] = \left[\frac{\partial B_{mu,1}(\xi)}{\partial\xi}.B_{nu,j}(\eta)\right]^T.\left[\frac{\partial B_{mu,1}(\xi)}{\partial\xi}.B_{nu,j}(\eta)\right] \quad \text{(A22a)}$$

$$\left[G_{u,2}\right] = \left[\frac{\partial B_{mu,1}(\xi)}{\partial\xi}.B_{nu,j}(\eta)\right]^T.\left[B_{mu,1}(\xi).\frac{\partial B_{nu,j}(\eta)}{\partial\eta}\right] \quad \text{(A22b)}$$

$$\left[G_{u,3}\right] = \left[B_{mu,1}(\xi).\frac{\partial B_{nu,j}(\eta)}{\partial\eta}\right]^T.\left[\frac{\partial B_{mu,1}(\xi)}{\partial\xi}.B_{nu,j}(\eta)\right] \quad \text{(A22c)}$$

$$\left[G_{u,4}\right] = \left[B_{mu,1}(\xi).\frac{\partial B_{nu,j}(\eta)}{\partial\eta}\right]^T.\left[B_{mu,1}(\xi).\frac{\partial B_{nu,j}(\eta)}{\partial\eta}\right] \quad \text{(A22d)}$$

Therefore the orientation of reference stresses σ_{xl}, σ_{yl} or τ_{xyl} must be defined according to the local orthogonal coordinates (x_L, y_L) of the finite element.

The Isoparametric solid finite element: In solid element, the strain-displacement equation will be:

$$\{\varepsilon\}=\begin{bmatrix}\varepsilon_x & \varepsilon_y & \varepsilon_z & \gamma_{xy} & \gamma_{xz} & \gamma_{yz}\end{bmatrix}^T=\begin{bmatrix}\frac{\partial u}{\partial x} & \frac{\partial v}{\partial y} & \frac{\partial w}{\partial z} & \left(\frac{\partial u}{\partial y}+\frac{\partial v}{\partial x}\right) & \left(\frac{\partial u}{\partial z}+\frac{\partial w}{\partial x}\right) & \left(\frac{\partial v}{\partial z}+\frac{\partial w}{\partial y}\right)\end{bmatrix}^T \tag{A23}$$

where x, y and z are the global orthogonal coordinates.

It is necessary to develop the relations of corresponding 3D-Jacobian matrix [J] and to establish its inverse, which can write the differential relations between the isoparametric coordinates (ξ,η,ζ) and global coordinates (x,y,z). Thus it will be easy to define the strain vector from the isoparametric coordinates.

$$\{\varepsilon\}=[A].[J']^{-1}.\begin{bmatrix}\frac{\partial u}{\partial \xi} & \frac{\partial v}{\partial \xi} & \frac{\partial w}{\partial \xi} & \frac{\partial u}{\partial \eta} & \frac{\partial v}{\partial \eta} & \frac{\partial w}{\partial \eta} & \frac{\partial u}{\partial \zeta} & \frac{\partial v}{\partial \zeta} & \frac{\partial w}{\partial \zeta}\end{bmatrix}^T=[B].\{\delta\} \tag{A24}$$

where

$$[A].[J']^{-1}=\begin{bmatrix}1&0&0&0&0&0&0&0&0\\0&0&0&0&1&0&0&0&0\\0&0&0&0&0&0&0&0&1\\0&1&0&1&0&0&0&0&0\\0&0&1&0&0&0&1&0&0\\0&0&0&0&0&1&0&1&0\end{bmatrix}.\begin{bmatrix}\frac{\partial \xi}{\partial x}&0&0&\frac{\partial \eta}{\partial x}&0&0&\frac{\partial \zeta}{\partial x}&0&0\\0&\frac{\partial \xi}{\partial x}&0&0&\frac{\partial \eta}{\partial x}&0&0&\frac{\partial \zeta}{\partial x}&0\\0&0&\frac{\partial \xi}{\partial x}&0&0&\frac{\partial \eta}{\partial x}&0&0&\frac{\partial \zeta}{\partial x}\\\frac{\partial \xi}{\partial y}&0&0&\frac{\partial \eta}{\partial y}&0&0&\frac{\partial \zeta}{\partial y}&0&0\\0&\frac{\partial \xi}{\partial y}&0&0&\frac{\partial \eta}{\partial y}&0&0&\frac{\partial \zeta}{\partial y}&0\\0&0&\frac{\partial \xi}{\partial y}&0&0&\frac{\partial \eta}{\partial y}&0&0&\frac{\partial \zeta}{\partial y}\\\frac{\partial \xi}{\partial z}&0&0&\frac{\partial \eta}{\partial z}&0&0&\frac{\partial \zeta}{\partial z}&0&0\\0&\frac{\partial \xi}{\partial z}&0&0&\frac{\partial \eta}{\partial z}&0&0&\frac{\partial \zeta}{\partial z}&0\\0&0&\frac{\partial \xi}{\partial z}&0&0&\frac{\partial \eta}{\partial z}&0&0&\frac{\partial \zeta}{\partial z}\end{bmatrix} \tag{A25}$$

The linear stress-strain relationship for solid finite element is:

$$\{\sigma\}=\begin{bmatrix}\sigma_{xx} & \sigma_{yy} & \sigma_{zz} & \tau_{xy} & \tau_{xz} & \tau_{yz}\end{bmatrix}^T=[D].\{\varepsilon\}=[D].[B].\{\delta\} \tag{A26}$$

The matrix [D] is the elasticity matrix defined for an isotropic material.
Consequently of developing the total energy, the stiffness matrix [K] can be evaluated from:

$$[K]=\int_{-1}^{+1}\int_{-1}^{+1}\int_{-1}^{+1}[B]^T.[D].[B].\det J(\xi,\eta,\zeta).d\xi.d\eta.d\zeta \tag{A27}$$

The load vector corresponding of self weight is:

$$\{F\}=\int_{-1}^{+1}\int_{-1}^{+1}\int_{-1}^{+1}\begin{bmatrix}\left[B_{mu,i}(\xi).B_{nu,j}(\eta).B_{lu,k}(\zeta)\right]^T & [0]^T & [0]^T\\ [0]^T & \left[B_{mv,i}(\xi).B_{nv,j}(\eta).B_{lv,k}(\zeta)\right]^T & [0]^T\\ [0]^T & [0]^T & \left[B_{mw,i}(\xi).B_{nw,j}(\eta).B_{lw,k}(\zeta)\right]^T\end{bmatrix}.\begin{Bmatrix}q_\xi\\q_\eta\\q_\zeta\end{Bmatrix}.\det J(\xi,\eta,\zeta).d\xi.d\eta.d\zeta \tag{A28}$$

The load vector for uniform or non-uniform surface loading may be defined one of the faces of the solid finite element. For example in the case of loading at a face ($\xi = -1$), we have:

$$\{F\} = \int_{-1}^{+1}\int_{-1}^{+1} \begin{bmatrix} \left[B_{nu,j}(\eta).B_{lu,k}(\zeta)\right]^T & [0]^T & [0]^T \\ [0]^T & \left[B_{nv,j}(\eta).B_{lv,k}(\zeta)\right]^T & [0]^T \\ [0]^T & [0]^T & \left[B_{nw,j}(\eta).B_{lw,k}(\zeta)\right]^T \end{bmatrix} . \begin{Bmatrix} q_\xi \\ q_\eta \\ q_\zeta \end{Bmatrix} . \det J(\eta,\zeta).d\eta.d\zeta \tag{A29}$$

In equation (A29), detJ(η,ζ) is corresponding to the 2D-Jacobian of the face loaded of a finite element.

The load vector for punctual loading (P_ξ,P_η,P_ζ) defined in a point with local coordinates (ξ_0, η_0, ζ_0) is:

$$\{F\} = \begin{Bmatrix} B_{mu,i}(\xi_0).B_{nu,j}(\eta_0).B_{lu,k}(\zeta_0).P_\xi \\ B_{mv,i}(\xi_0).B_{nv,j}(\eta_0).B_{lv,k}(\zeta_0).P_\eta \\ B_{mw,i}(\xi_0).B_{nw,j}(\eta_0).B_{lw,k}(\zeta_0).P_\zeta \end{Bmatrix} \tag{A30}$$

In the equations (A28-A30), a loading vector (q_x,q_y,q_z) or (P_x,P_y,P_z) defined in global system is transformed in a local system (q_ξ,q_η,q_ζ) or (P_ξ,P_η,P_ζ) respectively by application of a transformation matrix function. It is formed by inverse the isoparametric shape functions.

The mass matrix for a shell finite element with mass per unit volume ρ is given by:

$$[M] = \begin{bmatrix} [M_u] & [0] & [0] \\ [0] & [M_v] & [0] \\ [0] & [0] & [M_w] \end{bmatrix} \tag{A31}$$

The matrices [M_u], [M_u] and [Mw] are the mass matrices corresponding to the displacements u, v and w respectively.

$$[M_u] = \rho.\int_{-1}^{+1}\int_{-1}^{+1}\int_{-1}^{+1} \left[B_{mu,i}(\xi).B_{nu,j}(\eta).B_{lu,k}(\zeta)\right]^T.\left[B_{mu,i}(\xi).B_{nu,j}(\eta).B_{lu,k}(\zeta)\right].\det J(\xi,\eta,\zeta).d\xi.d\eta.d\zeta \tag{A32a}$$

$$[M_v] = \rho.\int_{-1}^{+1}\int_{-1}^{+1}\int_{-1}^{+1} \left[B_{mv,i}(\xi).B_{nv,j}(\eta).B_{lv,k}(\zeta)\right]^T.\left[B_{mv,i}(\xi).B_{nv,j}(\eta).B_{lv,k}(\zeta)\right].\det J(\xi,\eta,\zeta).d\xi.d\eta.d\zeta \tag{A32b}$$

$$[M_w] = \rho.\int_{-1}^{+1}\int_{-1}^{+1}\int_{-1}^{+1} \left[B_{mw,i}(\xi).B_{nw,j}(\eta).B_{lw,k}(\zeta)\right]^T.\left[B_{mw,i}(\xi).B_{nw,j}(\eta).B_{lw,k}(\zeta)\right].\det J(\xi,\eta,\zeta).d\xi.d\eta.d\zeta \tag{A32c}$$

The stability matrix corresponding to a compression stresses σ_{xx}, σ_{yy}, σ_{zz} are respectively:

$$[G_{xx}] = \sigma_{xx}.\int_{-1}^{+1}\int_{-1}^{+1}\int_{-1}^{+1} \begin{bmatrix} [A_1]^T & [A_2]^T & [A_3]^T & [0]^T & [0]^T & [0]^T & [0]^T & [0]^T & [0]^T \\ [0]^T & [0]^T & [0]^T & [A_4]^T & [A_5]^T & [A_6]^T & [0]^T & [0]^T & [0]^T \\ [0]^T & [0]^T & [0]^T & [0]^T & [0]^T & [0]^T & [A_7]^T & [A_8]^T & [A_9]^T \end{bmatrix} . \begin{bmatrix} \alpha_1 & 0 & 0 \\ \alpha_2 & 0 & 0 \\ \alpha_3 & 0 & 0 \\ 0 & \alpha_1 & 0 \\ 0 & \alpha_2 & 0 \\ 0 & \alpha_3 & 0 \\ 0 & 0 & \alpha_1 \\ 0 & 0 & \alpha_2 \\ 0 & 0 & \alpha_3 \end{bmatrix} .$$

$$\begin{bmatrix} \alpha_1 & \alpha_2 & \alpha_3 & 0 & 0 & 0 & 0 & 0 & 0 \\ 0 & 0 & 0 & \alpha_1 & \alpha_2 & \alpha_3 & 0 & 0 & 0 \\ 0 & 0 & 0 & 0 & 0 & 0 & \alpha_1 & \alpha_2 & \alpha_3 \end{bmatrix} . \begin{bmatrix} [A_1]^T & [0] & [0] \\ [A_2]^T & [0] & [0] \\ [A_3]^T & [0] & [0] \\ [0] & [A_4]^T & [0] \\ [0] & [A_5]^T & [0] \\ [0] & [A_6]^T & [0] \\ [0] & [0] & [A_7]^T \\ [0] & [0] & [A_8]^T \\ [0] & [0] & [A_9]^T \end{bmatrix} . \det J(\xi,\eta,\zeta).d\xi.d\eta.d\zeta \tag{A33}$$

$$\left[G_{yy}\right]=\sigma_{yy}.\int_{-1}^{+1}\int_{-1}^{+1}\int_{-1}^{+1}\begin{bmatrix}[A_1]^T & [A_2]^T & [A_3]^T & [0]^T & [0]^T & [0]^T & [0]^T & [0]^T & [0]^T\\ [0]^T & [0]^T & [0]^T & [A_4]^T & [A_5]^T & [A_6]^T & [0]^T & [0]^T & [0]^T\\ [0]^T & [0]^T & [0]^T & [0]^T & [0]^T & [0]^T & [A_7]^T & [A_8]^T & [A_9]^T\end{bmatrix}.\begin{bmatrix}\alpha_4 & 0 & 0\\ \alpha_5 & 0 & 0\\ \alpha_6 & 0 & 0\\ 0 & \alpha_4 & 0\\ 0 & \alpha_5 & 0\\ 0 & \alpha_6 & 0\\ 0 & 0 & \alpha_4\\ 0 & 0 & \alpha_5\\ 0 & 0 & \alpha_6\end{bmatrix}.$$

$$\begin{bmatrix}\alpha_4 & \alpha_5 & \alpha_6 & 0 & 0 & 0 & 0 & 0 & 0\\ 0 & 0 & 0 & \alpha_4 & \alpha_5 & \alpha_6 & 0 & 0 & 0\\ 0 & 0 & 0 & 0 & 0 & 0 & \alpha_4 & \alpha_5 & \alpha_6\end{bmatrix}.\begin{bmatrix}[A_1]^T & [0] & [0]\\ [A_2]^T & [0] & [0]\\ [A_3]^T & [0] & [0]\\ [0] & [A_4]^T & [0]\\ [0] & [A_5]^T & [0]\\ [0] & [A_6]^T & [0]\\ [0] & [0] & [A_7]^T\\ [0] & [0] & [A_8]^T\\ [0] & [0] & [A_9]^T\end{bmatrix}.\det J(\xi,\eta,\zeta).d\xi.d\eta.d\zeta \quad \text{(A34)}$$

$$\left[G_{zz}\right]=\sigma_{zz}.\int_{-1}^{+1}\int_{-1}^{+1}\int_{-1}^{+1}\begin{bmatrix}[A_1]^T & [A_2]^T & [A_3]^T & [0]^T & [0]^T & [0]^T & [0]^T & [0]^T & [0]^T\\ [0]^T & [0]^T & [0]^T & [A_4]^T & [A_5]^T & [A_6]^T & [0]^T & [0]^T & [0]^T\\ [0]^T & [0]^T & [0]^T & [0]^T & [0]^T & [0]^T & [A_7]^T & [A_8]^T & [A_9]^T\end{bmatrix}.\begin{bmatrix}\alpha_7 & 0 & 0\\ \alpha_8 & 0 & 0\\ \alpha_9 & 0 & 0\\ 0 & \alpha_7 & 0\\ 0 & \alpha_8 & 0\\ 0 & \alpha_9 & 0\\ 0 & 0 & \alpha_7\\ 0 & 0 & \alpha_8\\ 0 & 0 & \alpha_9\end{bmatrix}.$$

$$\begin{bmatrix}\alpha_7 & \alpha_8 & \alpha_9 & 0 & 0 & 0 & 0 & 0 & 0\\ 0 & 0 & 0 & \alpha_7 & \alpha_8 & \alpha_9 & 0 & 0 & 0\\ 0 & 0 & 0 & 0 & 0 & 0 & \alpha_7 & \alpha_8 & \alpha_9\end{bmatrix}.\begin{bmatrix}[A_1]^T & [0] & [0]\\ [A_2]^T & [0] & [0]\\ [A_3]^T & [0] & [0]\\ [0] & [A_4]^T & [0]\\ [0] & [A_5]^T & [0]\\ [0] & [A_6]^T & [0]\\ [0] & [0] & [A_7]^T\\ [0] & [0] & [A_8]^T\\ [0] & [0] & [A_9]^T\end{bmatrix}.\det J(\xi,\eta,\zeta).d\xi.d\eta.d\zeta \quad \text{(A35)}$$

The stability matrix corresponding to a shear stresses τ_{xy}, τ_{xz}, τ_{yz} are respectively:

$$\left[G_{xy}\right] = 2.\tau_{xy}.\int_{-1}^{+1}\int_{-1}^{+1}\int_{-1}^{+1}\begin{bmatrix} [A_1]^T & [A_2]^T & [A_3]^T & [0]^T & [0]^T & [0]^T & [0]^T & [0]^T & [0]^T \\ [0]^T & [0]^T & [0]^T & [A_4]^T & [A_5]^T & [A_6]^T & [0]^T & [0]^T & [0]^T \\ [0]^T & [0]^T & [0]^T & [0]^T & [0]^T & [0]^T & [A_7]^T & [A_8]^T & [A_9]^T \end{bmatrix}.\begin{bmatrix} \alpha_1 & 0 & 0 \\ \alpha_2 & 0 & 0 \\ \alpha_3 & 0 & 0 \\ 0 & \alpha_1 & 0 \\ 0 & \alpha_2 & 0 \\ 0 & \alpha_3 & 0 \\ 0 & 0 & \alpha_1 \\ 0 & 0 & \alpha_2 \\ 0 & 0 & \alpha_3 \end{bmatrix}.$$

$$\begin{bmatrix} \alpha_4 & \alpha_5 & \alpha_6 & 0 & 0 & 0 & 0 & 0 & 0 \\ 0 & 0 & 0 & \alpha_4 & \alpha_5 & \alpha_6 & 0 & 0 & 0 \\ 0 & 0 & 0 & 0 & 0 & 0 & \alpha_4 & \alpha_5 & \alpha_6 \end{bmatrix}.\begin{bmatrix} [A_1]^T & [0] & [0] \\ [A_2]^T & [0] & [0] \\ [A_3]^T & [0] & [0] \\ [0] & [A_4]^T & [0] \\ [0] & [A_5]^T & [0] \\ [0] & [A_6]^T & [0] \\ [0] & [0] & [A_7]^T \\ [0] & [0] & [A_8]^T \\ [0] & [0] & [A_9]^T \end{bmatrix}.\det J(\xi,\eta,\zeta).d\xi.d\eta.d\zeta \quad \text{(A36)}$$

$$\left[G_{xz}\right] = 2.\tau_{xz}.\int_{-1}^{+1}\int_{-1}^{+1}\int_{-1}^{+1}\begin{bmatrix} [A_1]^T & [A_2]^T & [A_3]^T & [0]^T & [0]^T & [0]^T & [0]^T & [0]^T & [0]^T \\ [0]^T & [0]^T & [0]^T & [A_4]^T & [A_5]^T & [A_6]^T & [0]^T & [0]^T & [0]^T \\ [0]^T & [0]^T & [0]^T & [0]^T & [0]^T & [0]^T & [A_7]^T & [A_8]^T & [A_9]^T \end{bmatrix}.\begin{bmatrix} \alpha_1 & 0 & 0 \\ \alpha_2 & 0 & 0 \\ \alpha_3 & 0 & 0 \\ 0 & \alpha_1 & 0 \\ 0 & \alpha_2 & 0 \\ 0 & \alpha_3 & 0 \\ 0 & 0 & \alpha_1 \\ 0 & 0 & \alpha_2 \\ 0 & 0 & \alpha_3 \end{bmatrix}.$$

$$\begin{bmatrix} \alpha_7 & \alpha_8 & \alpha_9 & 0 & 0 & 0 & 0 & 0 & 0 \\ 0 & 0 & 0 & \alpha_7 & \alpha_8 & \alpha_9 & 0 & 0 & 0 \\ 0 & 0 & 0 & 0 & 0 & 0 & \alpha_7 & \alpha_8 & \alpha_9 \end{bmatrix}.\begin{bmatrix} [A_1]^T & [0] & [0] \\ [A_2]^T & [0] & [0] \\ [A_3]^T & [0] & [0] \\ [0] & [A_4]^T & [0] \\ [0] & [A_5]^T & [0] \\ [0] & [A_6]^T & [0] \\ [0] & [0] & [A_7]^T \\ [0] & [0] & [A_8]^T \\ [0] & [0] & [A_9]^T \end{bmatrix}.\det J(\xi,\eta,\zeta).d\xi.d\eta.d\zeta \quad \text{(A37)}$$

$$\left[G_{yz}\right]=2.\tau_{yz}.\int_{-1}^{+1}\int_{-1}^{+1}\int_{-1}^{+1}\begin{bmatrix}[A_1]^T & [A_2]^T & [A_3]^T & [0]^T & [0]^T & [0]^T & [0]^T & [0]^T & [0]^T\\ [0]^T & [0]^T & [0]^T & [A_4]^T & [A_5]^T & [A_6]^T & [0]^T & [0]^T & [0]^T\\ [0]^T & [0]^T & [0]^T & [0]^T & [0]^T & [0]^T & [A_7]^T & [A_8]^T & [A_9]^T\end{bmatrix}.\begin{bmatrix}\alpha_4 & 0 & 0\\ \alpha_5 & 0 & 0\\ \alpha_6 & 0 & 0\\ 0 & \alpha_4 & 0\\ 0 & \alpha_5 & 0\\ 0 & \alpha_6 & 0\\ 0 & 0 & \alpha_4\\ 0 & 0 & \alpha_5\\ 0 & 0 & \alpha_6\end{bmatrix}.$$

$$\begin{bmatrix}\alpha_7 & \alpha_8 & \alpha_9 & 0 & 0 & 0 & 0 & 0 & 0\\ 0 & 0 & 0 & \alpha_7 & \alpha_8 & \alpha_9 & 0 & 0 & 0\\ 0 & 0 & 0 & 0 & 0 & 0 & \alpha_7 & \alpha_8 & \alpha_9\end{bmatrix}.\begin{bmatrix}[A_1]^T & [0] & [0]\\ [A_2]^T & [0] & [0]\\ [A_3]^T & [0] & [0]\\ [0] & [A_4]^T & [0]\\ [0] & [A_5]^T & [0]\\ [0] & [A_6]^T & [0]\\ [0] & [0] & [A_7]^T\\ [0] & [0] & [A_8]^T\\ [0] & [0] & [A_9]^T\end{bmatrix}.\det J(\xi,\eta,\zeta).d\xi.d\eta.d\zeta \quad (A38)$$

where

$$\begin{bmatrix}\alpha_1 & \alpha_2 & \alpha_3\\ \alpha_4 & \alpha_5 & \alpha_6\\ \alpha_7 & \alpha_8 & \alpha_9\end{bmatrix}=\begin{bmatrix}\frac{\partial\xi}{\partial x} & \frac{\partial\eta}{\partial x} & \frac{\partial\zeta}{\partial x}\\ \frac{\partial\xi}{\partial y} & \frac{\partial\eta}{\partial y} & \frac{\partial\zeta}{\partial y}\\ \frac{\partial\xi}{\partial z} & \frac{\partial\eta}{\partial z} & \frac{\partial\zeta}{\partial z}\end{bmatrix}=\left[J\right]^{-1} \quad (A39)$$

and

$$A_1=\frac{\partial B_{mu,i}(\xi)}{\partial\xi}.B_{nu,j}(\eta).B_{lu,k}(\zeta),\ A_2=B_{mu,i}(\xi).\frac{\partial B_{nu,j}(\eta)}{\partial\eta}.B_{lu,k}(\zeta),\ A_3=B_{mu,i}(\xi).B_{nu,j}(\eta).\frac{\partial B_{lu,k}(\zeta)}{\partial\zeta}$$

$$A_4=\frac{\partial B_{mv,i}(\xi)}{\partial\xi}.B_{nv,j}(\eta).B_{lv,k}(\zeta),\ A_5=B_{mv,i}(\xi).\frac{\partial B_{nv,j}(\eta)}{\partial\eta}.B_{lv,k}(\zeta),\ A_6=B_{mv,i}(\xi).B_{nv,j}(\eta).\frac{\partial B_{lv,k}(\zeta)}{\partial\zeta}$$

$$A_7=\frac{\partial B_{mw,i}(\xi)}{\partial\xi}.B_{nw,j}(\eta).B_{lw,k}(\zeta),\ A_8=B_{mw,i}(\xi).\frac{\partial B_{nw,j}(\eta)}{\partial\eta}.B_{lw,k}(\zeta),\ A_9=B_{mw,i}(\xi).B_{nw,j}(\eta).\frac{\partial B_{lw,k}(\zeta)}{\partial\zeta} \quad (A40)$$

Results of integration in bernstein basis functions: The numerical integrals appearing in calculus matrices and vectors are easily performed using directly the algebraic scheme of Bernstein polynomials corresponding for isoparametric one dimension finite element. Then it is easy to establish 'exact' integrals results applied in the components of matrices and vectors. The results of these integrals are as follows:

$$\int_{-1}^{+1}x^n.B_{m,i}(x).dx=\left(\frac{1}{2}\right)^{m-1}.(m-1)!.\left(\sum_{k=0}^{m-1}\left(\frac{(1)^{k+n+1}-(-1)^{k+n+1}}{k+n+1}\right).\left(\sum_{p=\sup(0,k-i+1)}^{\inf(m-i,k)}\left(\frac{(-1)^{2m-2i+p}}{p!.(m-i-p)!.(k-p)!(i-1-k+p)!}\right)\right)\right) \quad (A41)$$

$$\int_{-1}^{+1} x^n.B_{m_1,i}(x).B_{m_2,j}(x).dx = \left(\frac{1}{2}\right)^{m_1+m_2-2}.(m_1-1)!.(m_2-1)!.\left(\sum_{k=0}^{m_1+m_2-2}\left(\frac{(1)^{k+n+1}-(-1)^{k+n+1}}{k+n+1}\right).\left(\sum_{p=\sup(0,k-m_1+1)}^{\inf(k,m_2-1)}\left(\sum_{pp=\sup(0,k-p-i+1)}^{\inf(m_1-i,k-p)}\left(\frac{(-1)^{2m_1-2i+pp}}{pp!.(m_1-i-pp)!.(k-p-pp)!.(i-1-k+p+pp)!}\right)\right).\left(\sum_{pp=\sup(0,p-j+1)}^{\inf(m_2-j,p)}\left(\frac{(-1)^{2m_2-2j+pp}}{pp!(m_2-j-pp)!.(p-pp)!.(j-1-p+pp)!}\right)\right)\right)\right) \quad \text{(A42)}$$

$$\int_{-1}^{+1} x^n.\frac{\partial B_{m_1,i}(x)}{\partial x}.B_{m_2,j}(x).dx = \left(\frac{1}{2}\right)^{m_1+m_2-2}.(m_1-1)!.(m_2-1)!.\left(\sum_{k=0}^{m_1+m_2-3}\left(\frac{(1)^{k+n+1}-(-1)^{k+n+1}}{k+n+1}\right).\left(\sum_{p=\sup(0,k-m_1+2)}^{\inf(k,m_2-1)}\left(\sum_{pp=\sup(0,k-p-i+2)}^{\inf(m_1-i,k-p+1)}\left(\frac{(-1)^{2m_1-2i+pp}}{pp!.(m_1-i-pp)!.(k-p+1-pp)!.(i-2-k+p+pp)!}\right)\right).\left(\sum_{pp=\sup(0,p-j+1)}^{\inf(m_2-j,p)}\left(\frac{(-1)^{2m_2-2j+pp}}{pp!(m_2-j-pp)!.(p-pp)!.(j-1-p+pp)!}\right)\right).(k-p+1)\right)\right) \quad \text{(A43)}$$

$$\int_{-1}^{+1} x^n.\frac{\partial B_{m_1,i}(x)}{\partial x}.\frac{\partial B_{m_2,j}(x)}{\partial x}.dx = \left(\frac{1}{2}\right)^{m_1+m_2-2}.(m_1-1)!.(m_2-1)!.\left(\sum_{k=0}^{m_1+m_2-4}\left(\frac{(1)^{k+n+1}-(-1)^{k+n+1}}{k+n+1}\right).\left(\sum_{p=\sup(0,k-m_1+2)}^{\inf(k,m_2-2)}\left(\sum_{pp=\sup(0,k-p-i+2)}^{\inf(m_1-i,k-p+1)}\left(\frac{(-1)^{2m_1-2i+pp}}{pp!.(m_1-i-pp)!.(k-p+1-pp)!.(i-2-k+p+pp)!}\right)\right).\left(\sum_{pp=\sup(0,p-j+2)}^{\inf(m_2-j,p+1)}\left(\frac{(-1)^{2m_2-2j+pp}}{pp!(m_2-j-pp)!.(p+1-pp)!.(j-2-p+pp)!}\right)\right).(k-p+1).(p+1)\right)\right) \quad \text{(A44)}$$

$$\int_{-1}^{+1} x^n.\frac{\partial^2 B_{m_1,i}(x)}{\partial x^2}.B_{m_2,j}(x).dx = \left(\frac{1}{2}\right)^{m_1+m_2-2}.(m_1-1)!.(m_2-1)!.\left(\sum_{k=0}^{m_1+m_2-4}\left(\frac{(1)^{k+n+1}-(-1)^{k+n+1}}{k+n+1}\right).\left(\sum_{p=\sup(0,k-m_1+3)}^{\inf(k,m_2-2)}\left(\sum_{pp=\sup(0,k-p-i+3)}^{\inf(m_1-i,k-p+2)}\left(\frac{(-1)^{2m_1-2i+pp}}{pp!.(m_1-i-pp)!.(k-p+2-pp)!.(i-3-k+p+pp)!}\right)\right).\left(\sum_{pp=\sup(0,p-j+1)}^{\inf(m_2-j,p)}\left(\frac{(-1)^{2m_2-2j+pp}}{pp!(m_2-j-pp)!.(p-pp)!.(j-1-p+pp)!}\right)\right).(k-p+1).(k-p+2)\right)\right) \quad \text{(A45)}$$

$$\int_{-1}^{+1} x^n.\frac{\partial^2 B_{m_1,i}(x)}{\partial x^2}.\frac{\partial B_{m_2,j}(x)}{\partial x}.dx = \left(\frac{1}{2}\right)^{m_1+m_2-2}.(m_1-1)!.(m_2-1)!.\left(\sum_{k=0}^{m_1+m_2-5}\left(\frac{(1)^{k+n+1}-(-1)^{k+n+1}}{k+n+1}\right).\left(\sum_{p=\sup(0,k-m_1+3)}^{\inf(k,m_2-2)}\left(\sum_{pp=\sup(0,k-p-i+3)}^{\inf(m_1-i,k-p+2)}\left(\frac{(-1)^{2m_1-2i+pp}}{pp!.(m_1-i-pp)!.(k-p+2-pp)!.(i-3-k+p+pp)!}\right)\right).\left(\sum_{pp=\sup(0,p-j+2)}^{\inf(m_2-j,p+1)}\left(\frac{(-1)^{2m_2-2j+pp}}{pp!(m_2-j-pp)!.(p+1-pp)!.(j-2-p+pp)!}\right)\right).(k-p+1).(k-p+2)(p+1)\right)\right) \quad \text{(A46)}$$

$$\int_{-1}^{+1} x^n . \frac{\partial^2 B_{m_1,i}(x)}{\partial x^2} . \frac{\partial^2 B_{m_2,j}(x)}{\partial x^2} . dx = \left(\frac{1}{2}\right)^{m_1+m_2-2} . (m_1-1)! . (m_2-1)! . \left(\sum_{k=0}^{m_1+m_2-6} \left(\frac{(1)^{k+n+1} - (-1)^{k+n+1}}{k+n+1} \right) . \left(\sum_{p=\sup(0,k-m_1+3)}^{\inf(k,m_2-3)} \left(\sum_{pp=\sup(0,k-p-i+3)}^{\inf(m_1-i,k-p+2)} \left(\frac{(-1)^{2m_1-2i+pp}}{pp!.(m_1-i-pp)!.(k-p+2-pp)!.(i-3-k+p+pp)!} \right) \right) . \left(\sum_{pp=\sup(0,p-j+3)}^{\inf(m_2-j,p+2)} \left(\frac{(-1)^{2m_2-2j+pp}}{pp!(m_2-j-pp)!.(p+2-pp)!.(j-3-p+pp)!} \right) \right) . (k-p+1).(k-p+2)(p+1).(p+2) \right) \right) \right) \tag{A47}$$

The structural analysis programs are written in double-precision floating point with 16 digits. The stiffness matrix is positive defined. All the matrices are symmetric.

Boundary conditions and general constraints: For simply supported and clamped conditions, one extreme Bernstein polynomial and two extreme Bernstein polynomial are eliminated respectively whereas none is eliminated for the free end conditions.

In a composed structure, some elements may be connected back to each common interface: a common joint in frames elements, a common side in shells elements or a common surface in solids elements. This connection defines the continuities of displacements in interfaces. A transformation of the global stiffness matrix is done to satisfy this displacement compatibility conditions. Consequently the global stiffness matrix form is modified as shown in Fig. 4. Then the mass matrix [M] and the stability matrix [G] and the load vector {F} are be subjected to the same numerical transformation.

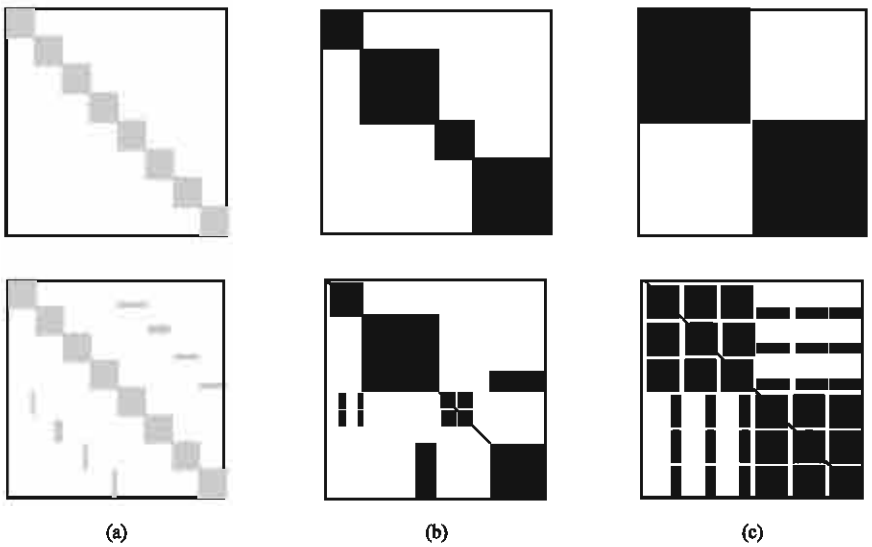

Fig. 4: Filling of the stiffness matrix before and after connection's transformation
a-Frame finite elements, b-Shell finite elements, c-Solid finite elements

NUMERICAL EXAMPLES

Initially, a conditioning number analysis is done for a simple beam to show a well-conditioned system of Bezier-Bernstein functions. Numerical solutions for several beams, shells and solids systems with various boundary conditions are given below to prove convergence.

Frame finite element systems

Conditioning number of one dimensional p-version functions: The conditioning number influences numerical round-off errors of linear problems. Among the various p-version approximations in current use, those based on Legendre, Legendre-Rodriguess, Chebyshev, Bézier-Bernstein, Lagrange, B3-Spline and sinusoidal polynomials are most common. Consider a simple finite element of length two units in the natural coordinate system ξ with simply supported ends in the two cases of axial and bending loading. The Bézier-Bernstein function has an interesting result. The element conditioning number increases for higher degree of functions (Fig. 5).

Axial-bending convergence of a simple beam: A simple beam clamped at one end and free at the other with simultaneous axial and perpendicular trapezoidal loading as shown in Fig. 6 is studied. To compare the efficiency of the Bézier element, it is observed that a fourth order is needed in an axial displacement function and a sixth order in bending displacement function, as shown in Fig. 7. This result is obvious when considering the type of applied loading.

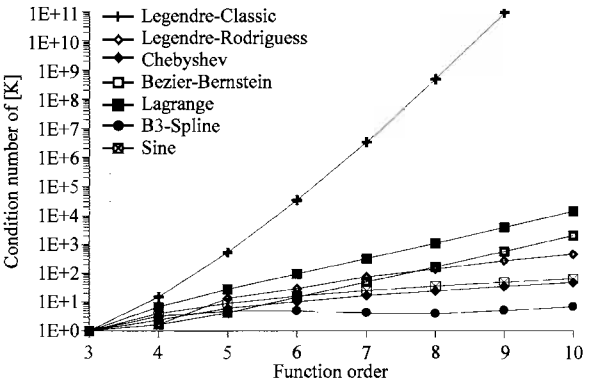

(a) Axial case

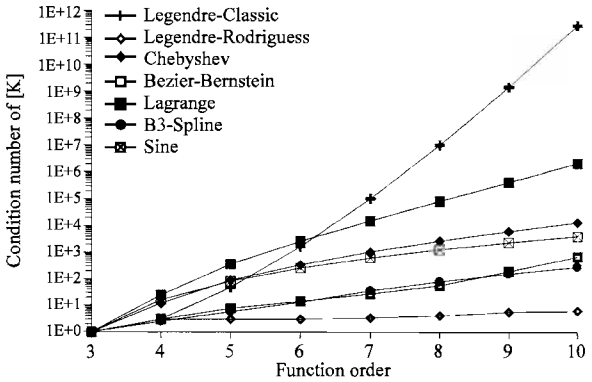

(b) Bending case

Fig. 5: Element conditioning number vs. function order for axial and bending cases

Free vibration of a stepped beam: Consider the free vibration of a stepped beam as shown in Fig. 8, clamped at one end, free at the other and with simple support at each section of discontinuity in cross section. A Bézier finite element is used in each span. Only axial and bending displacements in one plan are considered. Table 1 shows the highest four first period of free vibration. It is observed that results are accurate to the seventh order of

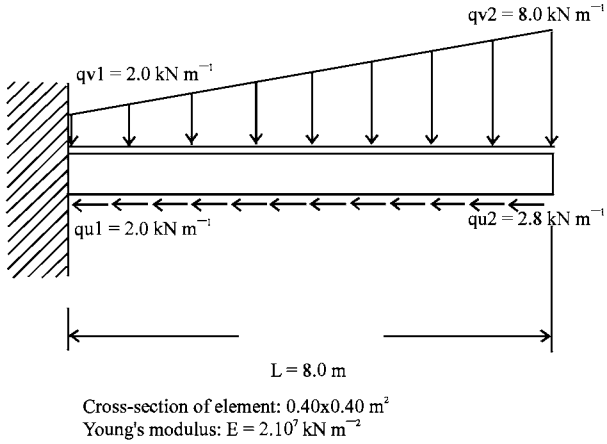

Fig. 6: Beam clamped-free ends

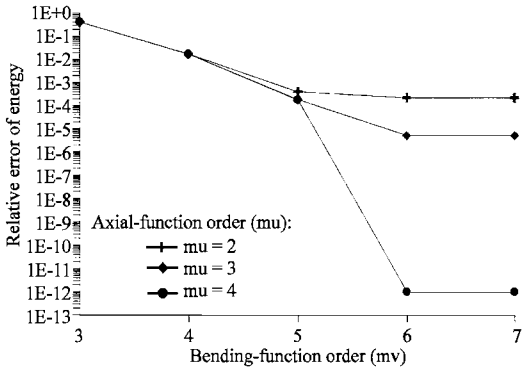

Fig. 7: Convergence of energy relative error

Table 1: The highest four first period of stepped beam shown in Fig. 8

Orders m_u, m_v	No. of Dof	Free vibration periods (sec) T_1	T_2	T_3	T_4
4	17	0.05500	0.01389	0.01016	0.00526
5	23	0.05521	0.01389	0.01150	0.00823
6	29	0.05523	0.01389	0.01152	0.00825
7	35	0.05523	0.01389	0.01153	0.00828
8	41	0.05523	0.01389	0.01153	0.00828
h-FEM	236	0.05523	0.01389	0.01153	0.00829

Bézier finite element. The conventional finite element method has the same accuracy with more than six times of dof's number. Hence the Bézier finite element is more efficient.

Buckling of clamped-simply supported beam: In order to study the rate of convergence of the buckling load factor of members, the Bézier finite element method has been applied to a clamped-simply supported beam (Fig. 9). The results are compared with the Euler buckling loads factors. It is observed that in order to achieve an error of less than 1% for the fourth first buckling loads factors, the 11th order of Bézier finite element are required. For the 14th order, the relative error decreases to 1.10^{-5}, as shown in Table 2.

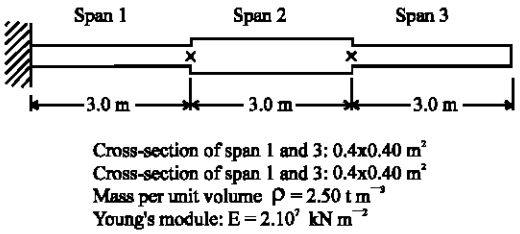

Fig. 8: Stepped beam clamped-free and with intermediate simple supports

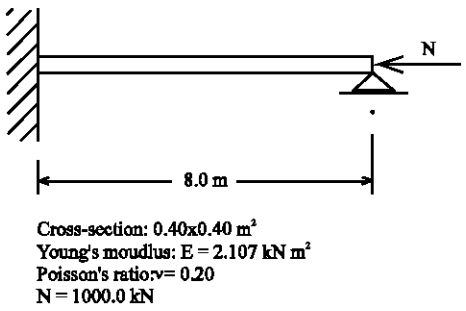

Fig. 9: Clamped-simply supported beam with intermediate simple supports

Table 2: The lowest four first buckling load factor of beam shown in Fig. 9

	Buckling load factor			
Order m_v	λ_1	λ_2	λ_3	λ_4
4	19.99999	3199.998	-	-
5	13.94578	71.38750	3199.998	-
6	13.52384	43.95395	175.8554	3199.999
7	13.46287	40.64799	95.39440	362.49461
8	13.46061	39.79632	83.43067	176.13758
9	13.46048	39.78683	79.98489	144.92428
10	13.46047	39.78683	79.39119	134.95862
11	13.46048	39.78635	79.27867	132.62035
12	13.46048	39.78632	79.26778	132.01190
13	13.46048	39.78632	79.26659	131.92069
14	13.46048	39.78633	79.26657	131.90653
Theory	13.46048	39.78634	79.26657	131.90520

Shell finite element systems

Membrane and flexural behaviour of square plate with simply supported edges: A square plate with simply supported edges as shown in Fig. 10 is analyzed. The loading is defined both normal to the plane and at the in-plane of the plate. It is loaded by a triangular loading in x direction, with a maximum of 10 kN m^{-2} at the right side. The results of displacement and forces at the selected point A (a plate centre) shows that the relative error is less than 1% for a 7th order of Bézier finite element in each direction of the element, as shown in Table 3.

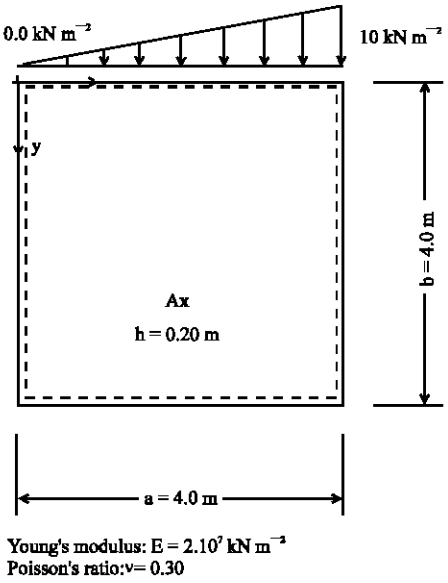

Fig. 10: Simply supported square plate

Table 3: Convergence of membrane and flexural behaviour

m_u, n_u	Membrane behaviour		Flexural behaviour	
m_v, n_v	u_A	$N_{x,A}$	w_A	$M_{x,A}$
m_w, n_w	($.10^{-6}$m)	(kN m^{-1})	($.10^{-4}$m)	(kN m^{-1})
3	2.1065	0.000	3.1023	2.954
4	2.1650	1.884	3.1023	2.954
5	2.0555	1.596	3.5803	4.001
6	2.0499	1.676	3.5803	4.001
7	2.0462	1.667	3.5487	3.831
8	2.0454	1.679	3.5487	3.831
9	2.0452	1.674	3.5488	3.831
10	2.0451	1.677	3.5488	3.831
11	2.0451	1.675	3.5489	3.831
12	2.0451	1.676	3.5489	3.831

Flexural free vibration of square plates and skew plate of various boundary conditions: A number of square plates with various boundary conditions and a skew plate were analyzed using a single finite element with various Bézier orders in both directions. Table 4 shows the results for the lowest six natural frequencies. For the square plate

Table 4: Natural frequencies of square plates and skew plate with various boundary conditions

	Natural frequencies $\lambda_i = \omega_i.a^2.\sqrt{\rho.h/D}$					
Mode sequence	λ_1	λ_2	λ_3	λ_4	λ_5	λ_6
S-S-S-S square plate:						
Leissa (1973)	19.74	49.35	49.35	78.96	98.70	98.70
Warburton (1954)	19.74	49.35	49.35	78.95	98.69	98.69
Finite strip method (Cheung and Cheung, 1971) (80 dof)	19.74	49.32	49.34	78.91	98.64	98.68
Spline finite strip method (Fan and Au, 1984) (112 dof)	19.74	49.36	49.38	78.98	98.80	99.21
Spline finite element method (Leung, 1990) (64 dof)	19.74	49.36	49.36	78.98	98.95	98.95
Bézier finite element method (m = n = 9, 49 dof)	19.74	49.35	49.35	78.96	98.71	98.71
F-S-F-S square plate:						
Leissa (1973)	9.63	16.13	36.73	38.95	46.74	70.74
Warburton (1954)	9.87	17.17	38.12	39.48	48.45	74.02
Finite strip method (Cheung and Cheung, 1971) (80 dof)	9.87	16.91	38.11	39.49	47.72	74.03
Spline finite strip method (Fan and Cheun, 1984) (144 dof)	9.80	17.02	37.90	39.38	48.03	72.82
Spline finite element method (Leung and Au, 1990) (80 dof)	9.63	16.14	36.74	38.97	46.76	70.78
Bézier finite element method (m = n = 8, 48 dof)	9.63	16.13	36.73	38.95	46.74	70.74
C-C-C-F square plate:						
Leissa (1973)	24.02	40.04	63.49	76.76	80.71	116.80
Warburton (1954)	24.60	41.50	64.50	77.99	83.53	119.30
Finite strip method (Cheung and Cheung, 1971) (80 dof)	24.11	40.66	63.61	77.32	81.77	118.60
Spline finite strip method (Fan and Cheung, 1984) (98 dof)	24.35	40.66	63.90	77.41	81.66	118.20
Spline finite element method (Leung and Au, 1990) (48 dof)	23.95	40.03	63.35	76.85	80.70	116.90
Bézier finite element method (m = n = 9, 35 dof)	23.93	40.01	63.28	76.73	80.62	116.70
Corner supported square plate:						
Leissa (1973)	7.12	15.77	15.77	19.60	38.44	44.40
Spline finite strip method (Fan and Cheung, 1984) (135 dof)	7.11	15.77	15.77	19.58	38.43	44.37
Spline finite element method (Leung and Au, 1990) (79 dof)	7.11	15.77	15.77	19.60	38.43	44.37
Bézier finite element method (m = n = 8, 60 dof)	7.11	15.77	15.77	19.60	38.43	44.37
S-S-S-S skew plate ($\beta = 45°$, a/b = 1.0):						
Liew *et al.* (1998) (p = 14, 120 dof)	35.33	66.27	100.50	108.40	140.80	168.30
Hierarchical F.E.M.(Bardell, 1992) (m = n = 14,144dof)	35.04	66.28	100.30	107.60	140.80	168.20
Bézier finite element method (m = n = 12, 100 dof)	35.33	66.28	100.40	108.30	140.80	168.30

cases, the results are compared with those given by Leissa (1973), Warburton (1954), the finite strip solution by Cheung and Cheung (1971), the spline finite strip solution by Fan and Cheung (1984) and spline finite element method by Leung and Au (Leung, 1990). For the skew plate's case, the results are compared with those given by Liew (1998) and Bardell (1992). Hence it is observed that the Bézier finite element method is as efficient as the other methods.

Buckling of rectangular plate with various boundary conditions: A few simple examples are used to investigate the convergence of the buckling loads of plates using Bézier finite element method with increasing the Bézier-Bernstein's orders. Some rectangular plates with simply supported and clamped edges are subjected to uniform longitudinal compression or shear. The resulting local buckling coefficients K are set out in Table 5 and are compared with the values given in Ref. 24 and 25 (Lau *et al.*, 1986 and Bulson, 1972). The buckling coefficients converge rapidly when the order number on Bézier finite element is increased. For the case of longitudinal compression, the relative error is less than 1% when the Bézier's order is equal to 7. For the case of shear, the convergence is slower; the relative error is less than 1% when the Bézier's order is equal to 10. Compared to the spline finite strip method, the Bézier finite element method gives good agreement.

Table 5: Buckling coefficients (K_i) of plates subjected to compression and shear

		Buckling coefficients $K_i = \lambda_i.\left(\frac{12.(1-\nu^2)}{\pi^2.E}.\left(\frac{b}{h}\right)^2\right)$		
		Longitudinal compression		Shear
No. of Bezier's order (m_w,n_w)	No. of DOFs	Simply supported (a/b = 1.00)	Simply supported (a/b = 1.00)	Clamped supported (a/b = 5.00)
4	4	5.307	9.354	21.151
5	9	4.786	8.677	10.337
6	16	4.695	8.294	7.010
7	25	4.019	7.918	6.061
8	36	4.000	7.918	5.858
9	49	4.000	7.868	5.667
10	64	4.000	7.868	5.562
11	81	4.000	7.867	5.546
12	100	4.000	7.867	5.532
Spline F.S.M (Lau *et al.*,1986)	156	4.001	7.889	5.550
(Bulson, 1972)		4.000	7.880	5.500

Continuity requirements: It is interesting to observe the effect of the variation of the Bézier finite elements degrees on the continuity of displacements across interfaces. This problem is treated by a parametric analysis of Bézier finite

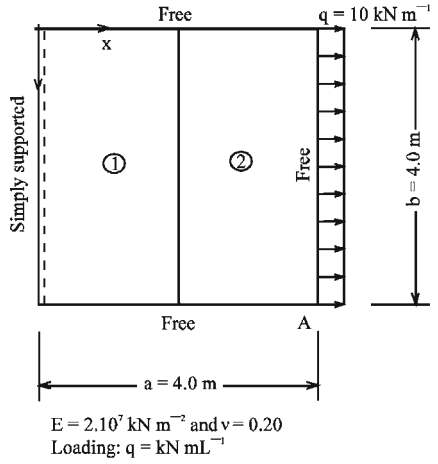

Fig. 11: A square plate with linear loading

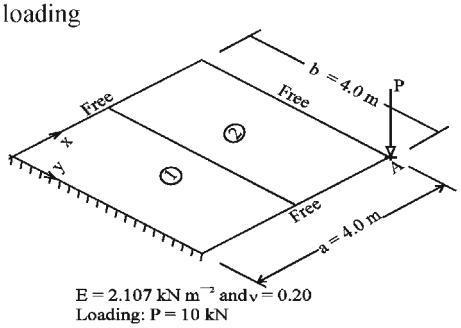

Fig. 12: A square shell with punctual loading

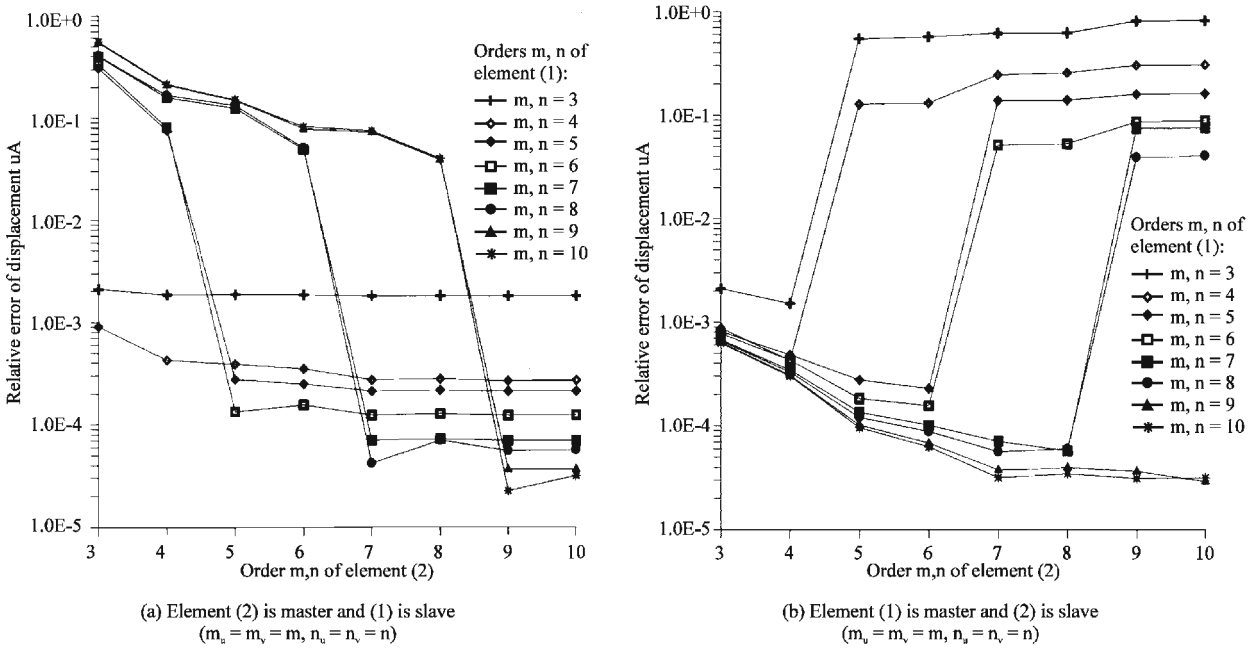

Fig. 13: Relative error of displacement (u_A) with various orders of two finite elements

element degrees in then membrane case and flexural case respectively as shown in Fig. 11 and 12. In the case of a plate with an in-plane loading, if the element (2) is master and element (1) is slave; a large relative error is shown when the difference of the order's finite elements increases. The precision improves when the orders of the

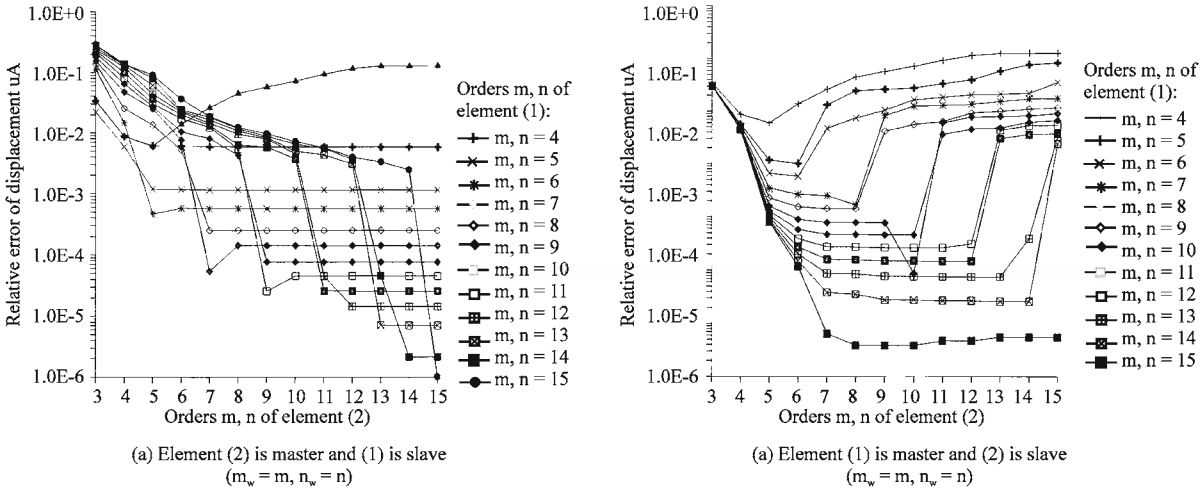

Fig. 14: Relative error of displacement (w_A) with various orders of two finite elements

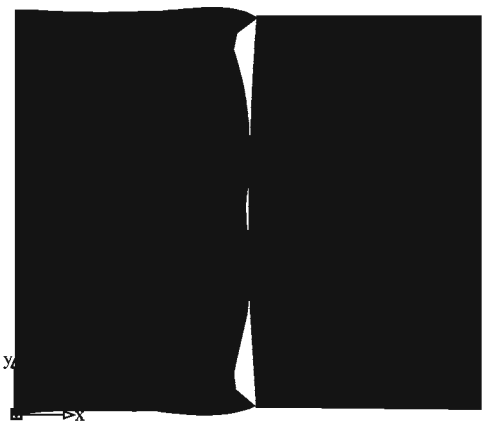

Fig. 15: Tear in plate shown in Fig. 11
(Case m,n (2)<m,n(1))

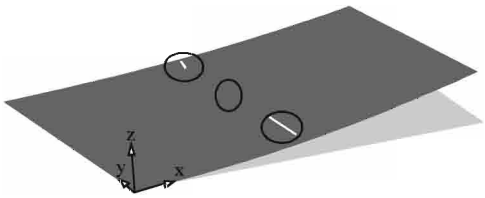

Fig. 16: Tear in shell shown in Fig. 12
(Case m,n (2)<m,n(1))

two finite elements increase. If the element (1) is master and element (2) is slave and the orders of the second element is superior to the first element, we remark that the relative error is large as shown in Fig. 13 and a discontinuity of displacements in the interface as shown in Fig. 15. The same results are collected in the case of flexural state as shown in Fig. 14 and 16. We can conclude that the orders of the master finite element must

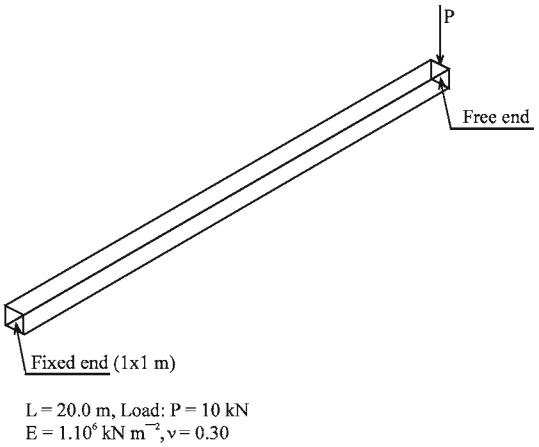

Fig. 17: A 3D-view of a fixed-free beam

be superior to the orders of the slave element to preserving the continuity of displacements.

Solid finite element systems

A static analysis of a fixed-free beam: A fixed-free beam submitted to a punctual load at the free end as shown in Fig. 17 is studied. It is observed that for transverse orders n and l greater than 2, the relative error of energy is less than 1% for a longitudinal order m greater than 8. The convergence is faster in the transverse direction from the third order.

A flexural free vibration of thin and thick square plate and skew plate with various boundary conditions: A number of square plates with various boundary conditions and a skew plate were analyzed using a single solid finite element with various Bézier orders in three

Table 6: Natural frequencies of square plate and skew plate of various boundary conditions (v = 0.30)

	Natural frequencies $\lambda_i = \omega_i . a^2 . \sqrt{\rho . h / D}$			
Mode sequence	λ_1	λ_2	λ_3	λ_4
S-C-S-C thin square plate (h/a = 0.05):				
Liew *et al.* (1998) (p = 14, 120 dof)	26.65	49.06	59.12	78.69
Bézier finite element method (m = n = 10, l = 4, 912 dof)	26.46	47.94	58.77	77.01
C-C-C-C thick square plate (h/a = 0.20):				
Liew *et al.* (1998) (p = 14, 360 dof)	26.46	46.14	46.14	61.94
Bézier finite element method (m = n = 10, l = 4, 768 dof)	26.98	47.27	47.27	61.96
S-F-S-F thin skew plate (β = 45°, a/b = 1.0 (h/a = 0.05)):				
Liew *et al.* (1998) (p = 14, 120 dof)	15.15	18.71	36.94	52.24
Bézier finite element method (m = n = 10, l = 4, 960 dof)	14.49	18.76	37.22	53.54
C-C-C-C thick skew plate (β = 45°, a/b = 1.0 (h/a = 0.20)):				
Liew *et al.* (1998) (p = 14, 360 dof)	41.05	58.25	74.44	76.89
Bézier finite element method (m = n = 10, l = 4, 768 dof)	42.15	59.99	71.97	76.82

directions. The simply supported boundary is defined by restraining the displacement-control point corresponding to the lower edge of plate. For the fixed boundary, all the displacements-control point of the boundary's face are restrained. Table 6 shows the results of the lowest six natural frequencies. For the thin and the thick plate's cases, the results are compared with those of Kirchhoff and Mindlin theories respectively given by Liew (Liew, 1998). Liew's results are determined by a p-version finite element method with 14th degree. Good agreement is observed in the selected cases knowing that two different approaches are used. The 4th transverse (l) order is sufficient for a good convergence.

A free vibration of a column-beam frame: A composed frame system (column-beam) is analysed. The system is modelled as three solid finite elements: column, node and beam as shown in Fig. 18. The second solid finite element 'node' is defined as master in the constraint declarations since it is common to both other finite elements. The ration length/cross section dimension is greater than 10. In the analysis, the transverse orders (n,l) are varied first

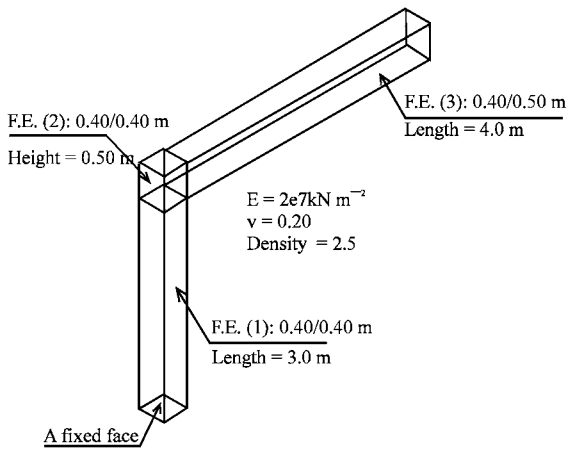

Fig. 18: A column-beam frame

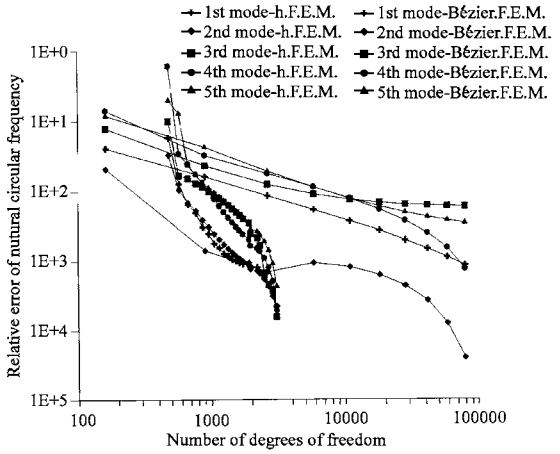

Fig. 19: Convergence of 5th lowest circular frequencies-of Bézier F.E.M. and classical F.E.M.

and the longitudinal orders of beam and column (m) are then varied in second. It should be noted that the second finite element 'node' have the same orders in three directions (m = n = l) necessary for a correct continuity of displacement already described in 4.2-d. A fast convergence of the results of natural circular frequencies is observed for transverse orders n and l from 4 and longitudinal order from 10. The 3D-view of the first 5 modes of free vibrations is shown in Fig. 20.

These results are compared with those of classical F.E.M. using an eight node finite element mesh. The Fig. 19 shows a rapid convergence of the Bézier F.E.M. for the 2nd mode, the relative error is less than 0.1% from 2646 dofs for the two methods. For the 1st mode, the relative error is less than 0.1% from 1632 dofs for the Bézier F.E.M. and from 79380 dofs for the classical F.E.M. For the other modes, the relative error is less than 0.1% from 2880 dofs for the Bézier F.E.M. and from 109512 dofs for the classical F.E.M. Thus compared to classical F.E.M., the Bézier F.E.M. is more powerful.

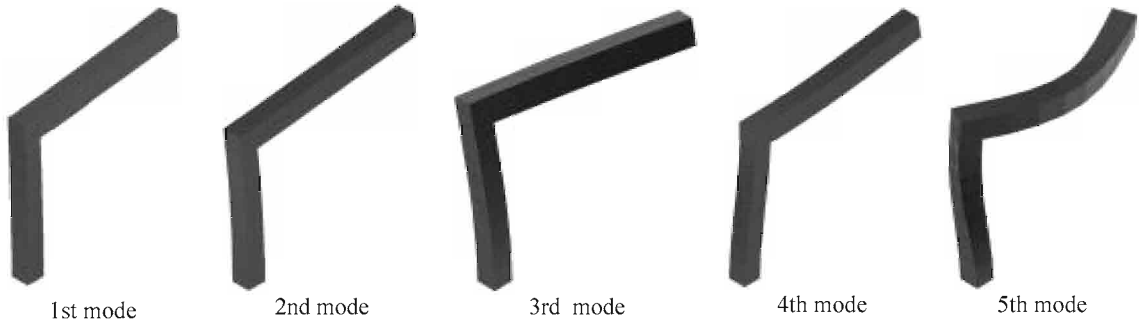

Fig. 20: 3-D view of free vibrations of the lowest fifth natural circular frequencies

Buckling of a clamped-free column subjected to compression: order to analyze the efficiency of the Bézier finite element method, the rate of convergence of the buckling stress is considered. The stability of a simple column, with the clamped-free ends and which is submitted to a longitudinal normal stress σ_{xx}, is analyzed (Fig. 21). The longitudinal orders (m) is varied with each cross-section orders (n,l). The Fig. 22 shows that from the

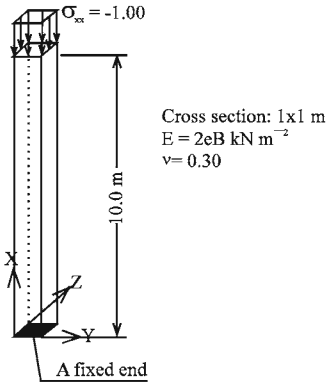

Fig. 21: A clamped-free column

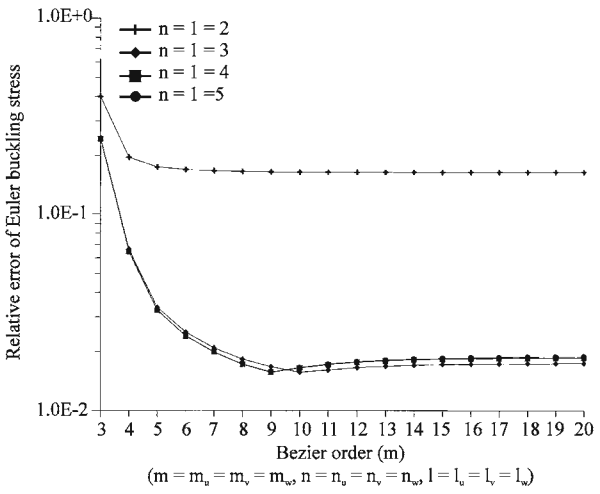

Fig. 22: Convergence of Euler buckling stress of column

third order for n and l is sufficient to model the transverse deformation. From a 10th longitudinal order, a convergence is shown with an asymptotic value of relative error of Euler buckling stress equal to 2%. In comparison with the one-dimensional model, this shift is due to the three-dimensional behaviour of the element.

CONCLUSIONS

In this study an implementation of a p-version FEM constructed from Bézier-Bernstein functions basis is presented. All numerical tools of isoparametric frame, shell and solid finite elements are established for elastic linear static, modal and stability analyses.

The Bézier-Bernstein functions properties bring to the FEM several advantages: flexibility, an efficient smoothing, a good conditioning, a simple boundary conditions construction, a simple construction of C^0 and C^1 continuous function of displacement between two finite elements, an exponential convergence by increasing the Bézier finite element order and a good accuracy.

Future work will include the implementation of an adaptive multi-level optimum-displacement algorithm.

REFERENCES

Antes, H., 1974. Bicubic fundamental splines in plate bending. Intl. J. Num. Meth. Eng., 8: 503-511.

Bardell, N.S., 1992. The free vibration of skew plates using the hierarchical finite element method. Computers and Structures, 45: 841-874.

Barth, W. and W. Stuzlinger, 1993. Efficient ray tracing for Bézier and B-spline surfaces. Computers and Graphics, 17: 423-430.

Bulson, P.S., 1970. The Stability of Flat Plates. Chatto and Windus, London.

Cheung, Y.K. and M.S. Cheung, 1971. Flexural vibration of rectangular and other polygonal plates. Proc. A.S.C.E., J. Eng. Mech. Div., 97: 391-411.

Demengel, G. and J.P. Pouget, 1998, Modèles de Bézier, des B-splines et des NURBS, Editions Ellipses.

Fan, S.C. and Y.K. Cheung, 1984. Flexural free vibration of rectangular plates with complex support conditions. J. Sound Vibration, 93: 81-94.

Farin, G., 1997. Curves and Surfaces for Computer Aided Geometric Design: A Practical Guide. London Academic Press, 4th Edn.

Farouki, R.T., 1981. On the stability of transformation between power and Bernstein polynomial forms. Computer Aided Geometric Design, 8: 29-36.

Fujii, F., 1981. Discrete and non-discrete mixed methods for plate bending analysis. Intl. J. Num. Meth. Eng., 17: 1843-1859.

Fujii, F., 1982. Fonctions spline aux noeuds multiples an analyse numérique des plaques: Flexion, Flambement et Vibration. Annales de l'Institut Technique du bâtiment et des travaux publics, 403: 91-102.

Hermann, T., 1996. On the stability of polynomial transformations between Taylor, Bézier and Hermite forms. Numerical algorithms, 13: 307-320.

Kagan, P., A. Fischer and P.Z. Bar-Yoseph, 1998. New B-spline finite element approach for geometrical design and mechanical analysis. Intl. J. Num. Meth. Eng., 41: 435-458.

Lau, S.C.W. and G.J. Hancock, 1986. Buckling of thin flat-walled structures by a spline finite strip method, Thin-Walled Struct., 4: 269-294.

Leissa, A.W., 1973. The free vibration of rectangular plates. J. Sound Vibration, 31: 257-293.

Leung, A.Y.T. and Au F.T.K., 1990, Spline finite elements for beam and plate. Computers and Structures, 37: 717-729.

Liew, K.M., C.M. Wang, Y. Xiang and S. Kitipornchai, 1998. Vibration of Mindlin Plates-Programming the p-version Ritz method, Elsevier.

Peano, A.G., 1975. Hiearchies of conforming finite elements. D.Sc. Thesis, Sever Institute of Technology, Washington University, St. Louis, MO.

Warburton, G.B., 1954. The vibration of rectangular plates. Proc. I. Mech. E., 168: 371-384.